

# The effective potential of the confinement order parameter in the Hamiltonian approach

Hugo Reinhardt and Jan Heffner

*Institut für Theoretische Physik, Universität Tübingen,  
Auf der Morgenstelle 14, 72076 Tübingen, Germany*

(Dated: June 1, 2021)

The effective potential of the order parameter for confinement is calculated for  $SU(N)$  Yang–Mills theory in the Hamiltonian approach. Compactifying one spatial dimension and using a background gauge fixing, this potential is obtained within a variational approach by minimizing the energy density for given background field. In this formulation the inverse length of the compactified dimension represents the temperature. Using Gaussian trial wave functionals we establish an analytic relation between the propagators in the background gauge at finite temperature and the corresponding zero-temperature propagators in Coulomb gauge. In the simplest truncation, neglecting the ghost and using the ultraviolet form of the gluon energy, we recover the Weiss potential. Neglecting the ghost and using for the gluon energy  $\omega(p)$  the approximate Gribov formula  $\omega(p) \simeq p + M^2/p$  one finds a critical temperature of  $\sqrt{3}M/\pi$ . We explicitly show that the omission of the ghost drastically increases the transition temperature. From the full non-perturbative potential (with the ghost included) we extract a critical temperature of the deconfinement phase transition of 269 MeV for the gauge group  $SU(2)$  and 283 MeV for  $SU(3)$ .

PACS numbers: 11.10.Wx, 11.15.-q, 12.38.Aw, 12.38.Lg

## I. INTRODUCTION

One of the major challenges of particle physics is the understanding of the deconfinement phase transition from the confined hadronic phase with chiral symmetry spontaneously broken to the deconfined quark gluon plasma with chiral symmetry restored. This transition is expected to be driven by the gluon dynamics, which suggests to investigate this transition first in pure Yang–Mills theory. In the absence of quarks the deconfinement phase transition is related to the center of the gauge group [1]: Center symmetry is realized in the low-temperature confining phase and spontaneously broken in the high-temperature deconfining phase. When quarks are included, center symmetry is explicitly broken and the deconfinement phase transition is expected to become a crossover.

Understanding the deconfinement phase transition requires non-perturbative methods. In quenched QCD reliable results have been obtained by means of the lattice simulations [2]. These methods become, however, extremely expensive when dynamical quarks are included and fail at large baryon densities due to the notorious fermion sign problem at non-vanishing chemical potential. Alternative non-perturbative methods, which are based on the continuum formulation of QCD are therefore desirable. In recent years substantial progress has been made within continuum approaches to QCD [3–6]. Among these is a variational approach to the Hamiltonian formulation of Yang–Mills theory in Coulomb gauge [6–8]. In this approach the energy density is minimized using Gaussian type ansätze for the Yang–Mills vacuum wave functional. Within the approach of Ref. [6] a decent description of the infrared sector of Yang–Mills theory was obtained [9–14]. Extension of this approach to

full QCD has shown that the coupling of the quarks to the transversal gluons amplifies the spontaneous breaking of chiral symmetry [15]. Recently this approach was also extended to finite temperatures by considering the grand canonical ensemble, making a suitable quasi-particle ansatz for the density operator and minimizing the free energy [16, 17]. In the present paper we present an alternative Hamiltonian approach to finite temperature Yang–Mills theory, which does not require an ansatz for the density operator. The finite temperature is introduced here by compactifying one spatial dimension. From the physical point of view this approach therefore addresses, strictly speaking, the Casimir problem. A summary of preliminary results obtained in this approach was reported in [18].

The ground state properties of a quantum field theory are usually studied by means of the Euclidean space functional integral. This approach, which is also the basis for lattice calculations, can be easily extended to finite temperatures by compactifying the Euclidean time axis, whence the momentum variable (energy) corresponding to the compactified Euclidean time becomes discrete with values given by multiples of  $2\pi$  times the temperature (Matsubara frequencies). Due to the  $O(4)$  symmetry of Euclidean quantum field theory (at zero temperature) all four Euclidean dimensions are equivalent and instead of compactifying the time one can equally well compactify one of the spatial dimensions. This procedure can be also applied to the Hamiltonian formulation of a quantum field theory. Thus, instead of considering the canonical or grand canonical ensemble of a theory, its extension to finite temperatures can be equally well obtained by considering the theory for one compactified spatial dimension and identifying the length of the compactified dimension with the inverse temperature. In the present paper we

apply this procedure to study Yang–Mills theory at finite temperature and, in particular, will investigate the deconfinement phase transition. To make contact with the previous Hamiltonian formulation of Yang–Mills theory in Coulomb gauge we use here a background gauge fixing, which reduces to Coulomb gauge for vanishing background field. We will consider a constant Abelian background field living in the Cartan subalgebra and being directed along the compact dimension. We will then calculate the energy density as a function of the background field and the length of the compactified dimension. As will be shown in Sect. II this quantity provides the finite-temperature effective potential of the Polyakov loop, which is the order parameter of confinement. From this potential the critical temperature of the deconfinement phase transition will be extracted.

The organization of the paper is as follows: In the next section we show how the effective potential of the Polyakov loop can be calculated in the Hamiltonian approach. In Sect. II A we discuss how a background field chose in the Cartan subalgebra and directed along a compactified dimension can figure as an order parameter for confinement alternativ to the Polyakov loop. In Sect. II B we show how in the Hamiltonian approach a Lorentz invariant quantum field theory can be extended to finite temperature by compactifying a spatial dimension. The upshot of Sect. II is that the effective potential of the confinement order parameter can be obtained in the Hamiltonian approach form the energy density calculated as a function of a constant background field living in the Cartan subalgebra and being directed along a compactified spatial dimension. The background field method is formulated in the Hamiltonian approach in Sect. III. In Sect. IV we develop the Hamiltonian approach in the presence of a background field in a background gauge. The crucial point is here the resolution of Gauss’ law. In the absence of the background field this approach reduces to the Hamiltonian approach in Coulomb gauge [6]. We also discuss here the choice of the variational wave functional required to ensure that the expectation value of the gauge field agrees with the background field. The Dyson–Schwinger equations (DSE) for the various propagators in the presence of a background field are derived in Sect. V. In Sect. VI we consider a constant background field living in the Cartan subalgebra of the gauge group and relate the solutions of the corresponding DSEs to the ones of the Hamiltonian approach in Coulomb gauge in the absence of the background field. For pedagogical reasons we develop the formalism for the gauge group  $SU(2)$  and present its extension to  $SU(N)$  in Sect. VI D. In Sect. VII we summarize the results obtained in the Hamiltonian approach in Coulomb gauge for the various propagators, which serve as input for the background field calculation of the effective potential of the Polyakov loop given in Sect. VIII. A short summary and our conclusions are given in Sect. IX. Some lengthy mathematical derivations are deferred to appendices.

## II. THE EFFECTIVE POTENTIAL OF THE CONFINEMENT ORDER PARAMETER IN THE HAMILTONIAN APPROACH

### A. The Polyakov loop potential

Consider Yang–Mills theory at finite temperatures and assume that the temperature is introduced by compactifying the euclidean time axis, identifying the length  $L$  of the compactified dimension with the inverse temperature. In the absence of fermions the finite-temperature Yang–Mills theory is invariant under gauge transformations  $U(x_0, \mathbf{x})$ , which are temporally periodic up to an element  $z_k$  of the center  $Z(N)$  of the gauge group  $SU(N)$

$$U(L, \mathbf{x}) = z_k(\mathbf{x})U(0, \mathbf{x}), \quad (1)$$

where the center element is given by

$$z_k = e^{-2\pi\tilde{\mu}_k} = e^{i\frac{2\pi}{N}k} \mathbb{1} \in Z(N), \quad k = 0, 1, \dots, N-1 \quad (2)$$

with  $\tilde{\mu}_k = \tilde{\mu}_k^a T_a$  being a co-weight vector. (We use antihermitean generators  $T_a$ .) The order parameter of confinement is the expectation value  $\langle P[A_0](\mathbf{x}) \rangle$  of the Polyakov loop [19]

$$P[A_0](\mathbf{x}) = \frac{1}{N} \text{tr} \mathcal{P} \exp \left( - \int_0^L dx_0 A_0(x_0, \mathbf{x}) \right). \quad (3)$$

This quantity can be related to the free energy  $F_q(\mathbf{x})$  of an isolated static (infinitely heavy) quark at space position  $\mathbf{x}$  by [1]<sup>1</sup>

$$\langle P[A_0](\mathbf{x}) \rangle = e^{-LF_q(\mathbf{x})} \quad (4)$$

and is entirely defined within pure Yang–Mills theory. Under gauge transformations satisfying Eq. (1) the Polyakov loop transforms as

$$P[A_0](\mathbf{x}) \rightarrow z_k P[A_0](\mathbf{x}) \quad (5)$$

and so does  $\langle P[A_0] \rangle \rightarrow z_k \langle P[A_0] \rangle$ . It follows that the order parameter  $\langle P[A_0] \rangle$  vanishes in the center symmetric confining phase, while  $\langle P[A_0] \rangle \neq 0$  in the deconfining phase with center symmetry broken.

In the continuum theory the Polyakov loop is most easily calculated in Polyakov gauge, defined by  $\partial_0 A_0 = 0$

---

<sup>1</sup> The phases of Yang–Mills theory can be alternatively distinguished by the “disorder” parameter of confinement, the ’t Hooft loop [20], which is dual to the temporal Wilson loop but can be used both at zero and finite temperature. Its continuum representation was derived in Ref. [21]. Evaluation of the ’t Hooft loop in the Hamiltonian approach in Coulomb gauge (at zero temperature) has given a perimeter law [11] as expected for the confined phase.

and  $A_0$  living in the Cartan subalgebra.<sup>2</sup> In this gauge the path ordering in Eq. (3) becomes irrelevant

$$P[A_0](\mathbf{x}) = \frac{1}{N} \text{tr} e^{-LA_0(\mathbf{x})} \quad (6)$$

and under a global center transformation (5)  $A_0$  transforms as

$$A_0 \rightarrow A_0 + \frac{2\pi}{L} \tilde{\mu}_k. \quad (7)$$

In Refs. [24, 25] it was shown that in this gauge the inequality

$$\langle P[A_0] \rangle \leq P[\langle A_0 \rangle] \quad (8)$$

holds, and furthermore that also  $P[\langle A_0 \rangle]$  vanishes in the confining phase. This establishes  $P[\langle A_0 \rangle]$  (alternative to  $\langle P[A_0] \rangle$ ) as an order parameter of confinement. Furthermore, due to the unique relation (6) between the gauge field  $A_0$  in Polyakov gauge and  $P[A_0]$ , instead of  $P[\langle A_0 \rangle]$  one can also use  $\langle A_0 \rangle$  itself as alternative order parameter of confinement. As a consequence the phase structure of finite temperature Yang–Mills theory can be extracted from the effective potential  $e[\langle A_0 \rangle]$  of  $\langle A_0 \rangle$ . By gauge invariance a non-vanishing  $\langle A_0 \rangle$  requires the presence of an external background field  $a$ . Choosing  $a$  to be constant and diagonal (thus being in the Polyakov gauge) and to satisfy  $a = \langle A_0 \rangle$  the background field  $a$  becomes an order parameter of confinement, whose value is determined by the minimum of the effective potential  $e[\langle A_0 \rangle = a]$ . Gauge invariance ensures that this potential is invariant under the  $Z(N)$  transformation (7)

$$e \left[ \langle A_0 \rangle + \frac{2\pi}{L} \tilde{\mu}_k \right] = e[\langle A_0 \rangle]. \quad (9)$$

This potential was first calculated in one loop perturbation theory in Ref. [26]. Corrections to this potential from the renormalization of the kinetic terms of the gauge field were calculated in Ref. [27]. It was found that  $e[a]$  has its minimum at  $\bar{a} = 0$ , so that  $\langle P \rangle \simeq P[\bar{a}] = 1$ , implying that the theory is in the deconfining phase with center symmetry broken. This is the expected behavior at high temperature, where the one-loop calculation is reliable. In the low temperature confined phase one expects that  $e[a]$  is minimal at “center symmetric configurations”  $\bar{a}$ , for which  $\langle P \rangle \simeq P[\bar{a}] = 0$ . Such a behavior was found e.g. in Ref. [25, 28], where the effective potential was determined non-perturbatively from a renormalization group flow equation.

<sup>2</sup> In Polyakov gauge topological defects like magnetic monopoles and center vortices occur [22, 23], which presumably are the “confiner” of the theory.

## B. Finite temperature from compactification of a spatial dimension

Obviously, the order parameter  $\langle P \rangle \simeq P[\langle A_0 \rangle]$  or  $\langle A_0 \rangle$  is not directly accessible in Weyl gauge  $A_0 = 0$ , which is assumed in the canonical quantization. However, by  $O(4)$  symmetry, all four Euclidean dimensions are equivalent and instead of compactifying the time, one can equally well introduce the temperature by compactifying one of the spatial dimension, say the  $x_3$ -axis, and consider  $\langle A_3 \rangle$  as an order parameter for confinement. This can be seen as follows:

Consider Yang–Mills theory at finite temperature  $L^{-1}$ , which is defined by the partition function

$$Z(L) = \text{Tr} e^{-LH(\mathbf{A})}. \quad (10)$$

Here  $H(\mathbf{A})$  is the usual Yang–Mills Hamiltonian defined by canonical quantization in Weyl gauge  $A_0 = 0$ . The partition function (10) can be equivalently represented by the Euclidean functional integral, see for example Ref. [22]

$$Z(L) = \int_{x^0 - \text{pbc}} \prod_{\mu} \mathcal{D}A_{\mu}(x) e^{-S[A]}, \quad (11)$$

where

$$S[A] = \int_{-L/2}^{L/2} dx^0 \int d^3x \mathcal{L}(A^{\mu}; x^{\mu}) \quad (12)$$

is the Euclidean action and the functional integration is performed over temporally periodic fields

$$A^{\mu}(L/2, \mathbf{x}) = A^{\mu}(-L/2, \mathbf{x}), \quad (13)$$

which is indicated in Eq. (11) by the subscript  $x^0 - \text{pbc}$ . This boundary condition is absolutely necessary at finite  $L$  but becomes irrelevant in the zero temperature ( $L \rightarrow \infty$ ) limit.

We perform now the following change of variables

$$\begin{aligned} x^0 &\rightarrow z^3 & A^0 &\rightarrow C^3 \\ x^1 &\rightarrow z^0 & A^1 &\rightarrow C^0 \\ x^2 &\rightarrow z^1 & A^2 &\rightarrow C^1 \\ x^3 &\rightarrow z^2 & A^3 &\rightarrow C^2. \end{aligned} \quad (14)$$

Due to the  $O(4)$  invariance of the Euclidean Lagrangian we have

$$\mathcal{L}(A^{\mu}, x^{\mu}) = \mathcal{L}(C^{\mu}, z^{\mu}) \quad (15)$$

and the partition function (11) can be rewritten as

$$Z(L) = \int_{z^3 - \text{pbc}} \prod_{\mu} \mathcal{D}C^{\mu}(z) e^{-\tilde{S}[C^{\mu}]}, \quad (16)$$

where the action is now given by

$$\tilde{S}[C^{\mu}] = \int dz^0 dz^1 dz^2 \int_{-L/2}^{L/2} dz^3 \mathcal{L}(C^{\mu}, z^{\mu}) \quad (17)$$

and the functional integration runs over fields satisfying periodic boundary condition in the  $z^3$ -direction

$$C^\mu(z^0, z^1, z^2, L/2) = C^\mu(z^0, z^1, z^2, -L/2). \quad (18)$$

We can now interpret  $z^0$  as time and  $\mathbf{z} = (z^1, z^2, z^3)$  as space coordinates and perform a usual canonical quantization in “Weyl gauge”  $C^0 = 0$ , interpreting  $\mathbf{C} = (C^1, C^2, C^3)$  as spatial coordinates of the gauge field, which are defined, however, not on  $\mathbb{R}^3$  but instead on  $\mathbb{R}^2 \times S^1$ . We obtain then the usual Yang–Mills Hamiltonian in which, however, the integration over  $z^3$  is restricted to the interval  $[-\frac{L}{2}, \frac{L}{2}]$ . Let us denote this Hamiltonian by  $\tilde{H}(\mathbf{C}, L)$ . Obviously  $\tilde{H}(\mathbf{C}, L \rightarrow \infty) = H(\mathbf{C})$ . Reversing the steps which lead from (10) to (11) and taking into account the irrelevance of the temporal boundary conditions in the functional integral for an infinite time-interval we obtain from Eq. (16) the alternative representation of the partition function

$$Z(L) = \text{Tr} e^{-\int dz^0 \tilde{H}(\mathbf{C}, L)} = \lim_{T \rightarrow \infty} \text{Tr} e^{-T \tilde{H}(\mathbf{C}, L)}. \quad (19)$$

Due to the infinite  $z^0$ -(time-)interval  $T \rightarrow \infty$  only the lowest eigenvalue of  $\tilde{H}(\mathbf{C}, L)$  contributes to the partition function  $Z(L)$ . The calculation of  $Z(L)$  is thus reduced to solving the Schrödinger equation  $\tilde{H}(\mathbf{C}, L)\psi(\mathbf{C}) = E\psi(\mathbf{C})$  for the vacuum state on the space manifold  $\mathbb{R}^2 \times S^1(L)$ , where  $S^1(L)$  is a circle with circumference  $L$ .

The upshot of the above consideration is that finite-temperature gauge theory can be described in the Hamiltonian approach by compactifying a spatial dimension and solving the corresponding Schrödinger equation for the vacuum sector. As the above derivation shows this equivalence holds for any  $O(4)$  invariant quantum field theory.

The above consideration for the partition function can be extended to the finite-temperature effective potential  $e[\langle A_0 \rangle]$ . One finds that  $e[\langle A_0 \rangle = a]$  can be calculated in the Hamiltonian approach from  $e[\langle A_3 \rangle = a]$  with the  $z^3$ -axis compactified. Furthermore, as shown in Ref. [29], in the Hamilton approach the effective potential  $e[\langle A_3 \rangle = a]$  is given by the energy density in the state that minimizes  $\langle H \rangle$  for given  $\langle A_3 \rangle$ . In this paper we calculate the effective potential  $e[\langle A_3 \rangle = a]$  in the Hamiltonian approach using the representation (19) of the partition function. In the spirit of the discussion given in Sect. II A we will refer to  $e[\langle A_3 \rangle]$  as the effective potential of the Polyakov loop.

A few comments are in order: In the present paper we use the Hamiltonian approach merely as a mathematical tool to calculate the effective potential of the background field at finite temperatures. As the previous considerations show, strictly speaking, time in the present approach is not the true time but a spatial dimension and the compactified spatial dimensions represents the time. Alternatively, interpreting the time of the present Hamiltonian approach as the true time the present approach actually describes Yang–Mills theory in a space with one

compactified spatial dimension and is thus reminiscent of the Casimir problem.

### III. THE BACKGROUND FIELD METHOD IN THE HAMILTONIAN APPROACH

Let  $\psi[A] = \langle A | \psi \rangle$  be the gauge invariant wave functional of the Yang–Mills vacuum. The generating functional of the Hamiltonian approach is then defined by

$$e^{W[j]} = \langle \psi | e^{\int \mathbf{j} \mathbf{A}} | \psi \rangle. \quad (20)$$

Fixing the gauge by the standard Faddeev–Popov method we have explicitly

$$e^{W[j]} = \int \mathcal{D}A \text{Det } \mathcal{M}[A] \delta(f^a[A]) e^{-S[A] + \int \mathbf{j} \mathbf{A}}. \quad (21)$$

Here we have rewritten the wave functional as

$$\psi[A] = \exp\left(-\frac{1}{2}S[A]\right) \quad (22)$$

and assumed that it is real. Furthermore

$$f^a[A] = 0 \quad (23)$$

is the gauge fixing constraint and

$$\mathcal{M}^{ab} = \frac{\delta f^a[A^U]}{\delta \Theta^b} \quad (24)$$

is the corresponding Faddeev–Popov kernel with

$$A^U = U^\dagger(\partial + A)U = U^\dagger D U, \quad U = \exp(-\Theta) \quad (25)$$

being the gauge transformation. Formally Eq. (21) looks like the standard Yang–Mills functional integral of the Lagrangian formulation in Euclidean space. However, in Eq. (21)  $S[A]$  is not the usual classical action and the functional integral runs over the spatial components of the gauge field only. In principle,  $S[A]$  is not known. However, in recent years there has been substantial progress in determining this wave functional approximately from a variational principle. Furthermore, in 2+1 dimension more detailed information on the Yang–Mills vacuum wave functional has been obtained from lattice studies [30] and strong coupling considerations [31, 32]. In the present paper we will use for  $S[A]$  the results of the variational calculations in Coulomb gauge carried out in Refs. [6, 9, 17]. For the moment let us assume that  $\psi[A]$  and thus  $S[A]$  is known. The similarity of Eq. (21) with the standard Lagrangian Yang–Mills functional integral allows us to apply the standard background field method [33] to simplify the evaluation of the effective action

$$\Gamma[\bar{A}] = \left(-W[j] + \int \mathbf{j} \bar{\mathbf{A}}\right)_{j=j(\bar{A})}, \quad \bar{A} = \frac{\delta W[j]}{\delta j}. \quad (26)$$

For this purpose we split the gauge field  $A$  into a background field  $a$  and a fluctuating part  $\mathcal{A}$

$$A = a + \mathcal{A}. \quad (27)$$

The gauge transformation (25) of the total gauge field  $A$  can be distributed among the background field  $a$  and the fluctuation  $\mathcal{A}$  in different ways. The two common and convenient possibilities are:

1. quantum gauge transformations, which leave the background field invariant

$$\begin{aligned} \delta_q a &= 0 \\ \delta_q \mathcal{A} &= [D, \delta\Theta] = [d + \mathcal{A}, \delta\Theta], \end{aligned} \quad (28)$$

where

$$d = \partial + a \quad (29)$$

is the covariant derivative with the background field

2. background gauge transformations

$$\begin{aligned} \delta_b a &= [d, \Theta] \\ \delta_b \mathcal{A} &= [\mathcal{A}, \Theta]. \end{aligned} \quad (30)$$

Following the standard background field method [33] we introduce the generating functional

$$e^{\tilde{W}[a, j]} = \int \mathcal{D}\mathcal{A} \text{Det } \tilde{\mathcal{M}}[A] \delta(\tilde{f}^a[A]) e^{-S[a + \mathcal{A}] + \int j\mathcal{A}}, \quad (31)$$

which explicitly depends on the background field  $a$  since the source couples only to the fluctuation  $\mathcal{A}$  and since the gauge fixing functional  $\tilde{f}^a[A]$  may depend on the background field. The action  $S[A] = S[a + \mathcal{A}]$  is, of course, invariant under both transformations (28), (30). It is, however, convenient to eliminate the gauge degrees of freedom by fixing the invariance with respect to the quantum gauge transformation (28). Then the Faddeev–Popov operator is given by

$$\tilde{\mathcal{M}}^{ab}[A] = \frac{\delta_q \tilde{f}^a[A]}{\delta\Theta^b}. \quad (32)$$

As is well known, the generating functional  $\tilde{W}[a, j]$  is invariant under the background gauge transformations (30) if the gauge fixing functional  $\tilde{f}^a[A]$  transforms covariantly under these transformations. A convenient gauge, which satisfies this requirement, is the background gauge

$$\tilde{f}^a[A] = [\mathbf{d}, \mathcal{A}] \equiv [\mathbf{d}, \mathbf{A} - \mathbf{a}] = 0, \quad (33)$$

for which the Faddeev–Popov operator (32) reads

$$\tilde{\mathcal{M}}[A] = -\hat{\mathbf{D}}\hat{\mathbf{d}}, \quad (34)$$

where the hat “ $\hat{\phantom{x}}$ ” denotes the adjoint representation of the gauge group and  $\hat{D}$  is the covariant derivative

$$\hat{D}^{ab} = \delta^{ab}\partial + \hat{A}^{ab}, \quad \hat{A}^{ab} = \hat{T}_c^{ab}A^c, \quad \hat{T}_c^{ab} = f^{acb} \quad (35)$$

with  $f^{abc}$  being the structure constants. This gauge is the 3-dimensional spatial analogue of the Landau-deWitt gauge. It is not difficult to see that in the background gauge (33) both the gauge constraint and the corresponding Faddeev–Popov determinant are invariant under the background transformation (30). Consequently the generating functional  $\tilde{W}[a, j]$  (31) and hence also the effective action

$$\tilde{\Gamma}[a, \bar{\mathcal{A}}] = \left( \tilde{W}[a, j] - \int_{j=j(\bar{\mathcal{A}})} \bar{\mathcal{A}}j \right), \quad \bar{\mathcal{A}} = \frac{\delta\tilde{W}[a, j]}{\delta j} \quad (36)$$

are invariant under the background transformation  $\delta_b$  (30). Furthermore, from the translation invariance of the integration measure  $\mathcal{D}\mathcal{A}$  follows that the true effective action  $\Gamma[\bar{\mathcal{A}}]$ , see Eq. (26), is related to  $\tilde{\Gamma}[a, \bar{\mathcal{A}}]$  by

$$\tilde{\Gamma}[a, \bar{\mathcal{A}}] = \Gamma[a + \bar{\mathcal{A}}] \quad (37)$$

and the classical fields are related by

$$\bar{A} = a + \bar{\mathcal{A}}. \quad (38)$$

Obviously the invariance of  $\tilde{\Gamma}[a, \bar{\mathcal{A}}]$  under the background transformation (30) ensures the gauge invariance of  $\Gamma[\bar{\mathcal{A}}]$ . In this paper we will determine the effective potential  $\Gamma[a] = \tilde{\Gamma}[a, \bar{\mathcal{A}} = 0]$  for a constant background field  $a$ .

#### IV. HAMILTONIAN APPROACH IN THE PRESENCE OF AN BACKGROUND FIELD

Below we develop the Hamilton approach to Yang–Mills theory in the presence of an external background field. This approach is an extension of the Hamiltonian formulation in Coulomb gauge [6, 34] and reduces to the latter when the background field is switched off. Although in the presence of the background field the Hamiltonian approach could, in principle, be also formulated in Coulomb gauge the use of the more general background gauge (33) turns out to be advantageous.

##### A. Generalities

To simplify the bookkeeping we will use the compact notation  $A_{k_1}^{a_1}(\mathbf{x}_1) = A(1)$  for colored Lorentz vectors like the gauge potential and an analogous notation for colored Lorentz scalars like the ghost  $C^{a_1}(\mathbf{x}_1) = C(1)$ . We also define in coordinate space

$$\delta(1, 2) = \delta^{a_1 a_2} \delta(\mathbf{x}_1 - \mathbf{x}_2). \quad (39)$$

A repeated label means summation over the discrete color (and Lorentz) indices along with integration over the  $d$  spatial coordinates

$$A(1)B(1) \equiv \int d^d x \sum_{k=1}^d \sum_{a=1}^{N_c^2-1} A_k^a(\mathbf{x}) B_k^a(\mathbf{x}). \quad (40)$$

Furthermore, indices will be suppressed when they can be easily restored from the context.

The usual canonical quantization of gauge theory assumes Weyl gauge  $A_0 = 0$  and results in a Hamiltonian

$$H[A] = \frac{1}{2} \left( g^2 \mathbf{\Pi}^2 + \frac{1}{g^2} \mathbf{B}[A]^2 \right), \quad (41)$$

where  $\mathbf{\Pi}(1) = -i\delta/\delta A(1)$  is the momentum operator and  $B[A]$  is the non-Abelian magnetic field. Here we have absorbed the coupling constant  $g$  in the gauge field,  $gA \rightarrow A$ . This Hamiltonian is invariant under time-independent gauge transformations. In Weyl gauge Gauss' law escapes the (Heisenberg) equation of motion and has to be imposed as a constraint on the wave functional

$$\hat{\mathbf{D}}\mathbf{\Pi}\psi[A] = \rho_{\text{ext}}\psi[A]. \quad (42)$$

Here  $\rho_{\text{ext}}$  is the charge density of external matter fields. Since  $\hat{\mathbf{D}}\mathbf{\Pi}$  is the generator of (time-independent) gauge transformations, in the absence of matter fields the wave functional has to be gauge invariant  $\psi[A^U] = \psi[A]$ .

We are interested here in the Yang–Mills vacuum in the presence of an external vector field  $a$ . Let  $|\psi_a\rangle$  denote the vacuum wave functional in the presence of the external field  $a$  and

$$\langle \dots \rangle_a := \langle \psi_a | \dots | \psi_a \rangle \quad (43)$$

the corresponding vacuum expectation value. We assume here that the states  $|\psi_a\rangle$  are properly normalized,  $\langle \psi_a | \psi_a \rangle = 1$ . In the absence of external fields the gauge invariance of the vacuum wave functional  $|\psi_0\rangle$  guarantees that the expectation value of all gauge dependent quantities vanishes. This refers, in particular, to the expectation value of the gauge field

$$\langle \psi_0 | A | \psi_0 \rangle = 0. \quad (44)$$

The background field assigns a prescribed expectation value to the gauge field. If  $\psi_0[A] = \langle A | \psi_0 \rangle$  denotes the gauge invariant vacuum wave functional in the absence of the background field (which necessarily satisfies Eq. (44)), then it is trivial to see by a change of variables that the wave functional

$$\psi_a[A] := \psi_0[A - a] \quad (45)$$

has the property that

$$\langle A \rangle_a = a. \quad (46)$$

Although the wave functional (45) satisfies (46), in general it will not minimize the energy under the constraint (46). The wave functional  $|\psi_a\rangle$  which minimizes the energy under the constraint (46)

$$\langle H \rangle_a \rightarrow \min, \quad \langle A \rangle_a = a \quad (47)$$

can be obtained from the constrained variational principle

$$\langle H - j(1)A(1) \rangle_a \rightarrow \text{extr}, \quad (48)$$

where  $j$  is a Lagrange multiplier chosen such that Eq. (46) is fulfilled.

## B. The background gauge fixed Hamiltonian

Instead of working with gauge invariant wave functionals, it is usually more convenient to fix the gauge, where those gauges are preferable which allow for an explicit resolution of Gauss' law. The price one pays for the gauge fixing is that the Hamiltonian acquires a more complicated, usually non-local form. A convenient gauge in this respect is Coulomb gauge [34]. However, in the present paper, where we are interested in the energy density of the vacuum in the presence of an external background field  $a$ , Coulomb gauge is not the optimal choice. In this case it is more convenient to choose the background gauge (33) which gauge fixes the fluctuating field  $\mathcal{A} = A - a$  with respect to the background field  $a$ .

In view of the gauge (33) it is appropriate to introduce generalized longitudinal and transversal projection operators

$$\hat{l}_{ij}(x) = \hat{d}_i \left( \hat{\mathbf{d}}\hat{\mathbf{d}} \right)^{-1} \hat{d}_j, \quad \hat{t}_{ij} = \hat{\delta}_{ij} - \hat{l}_{ij}, \quad \hat{\delta}_{ij}^{ab} = \delta^{ab} \delta_{ij}, \quad (49)$$

where

$$\hat{d}_i^{ab} = \delta^{ab} \partial_i + \hat{a}_i^{ab}, \quad \hat{a}_i^{ab} = f^{acb} a_i^c, \quad (50)$$

is the covariant derivative (34) with the total gauge field replaced by the background field. For a constant background field, these projectors have the same properties as the ordinary longitudinal and transversal projectors as far as their spatial indices are concerned. However, they are non-trivial matrices in color space. Using these projectors we split the gauge field and the momentum operator into ‘‘longitudinal’’ and ‘‘transversal’’ parts<sup>3</sup>

$$\begin{aligned} A &= A^{\parallel} + A^{\perp}, & A_i^{\parallel} &= \hat{l}_{ij} A_j \\ \Pi &= \Pi^{\parallel} + \Pi^{\perp}, & \Pi_i^{\parallel} &= \hat{l}_{ij} \Pi_j. \end{aligned} \quad (51)$$

The longitudinal part of the gauge field  $A^{\parallel}$  will be later eliminated by the background gauge fixing, Eq. (33), while the longitudinal part of the momentum operator  $\Pi^{\parallel}$  is eliminated by resolving Gauss' law (42), which can be explicitly done in the gauge (33) as we will show now.

Inserting Eq. (51) into Gauss' law (42) and solving for the longitudinal part of the momentum operator we find

$$\Pi^{\parallel} \psi = -\hat{d} \left( -\hat{\mathbf{D}}\hat{\mathbf{d}} \right)^{-1} \rho \psi, \quad (52)$$

where

$$\rho = \rho_{\text{ext}} + \rho_{\text{dyn}}[A] \quad (53)$$

<sup>3</sup> We keep here the terms ‘‘longitudinal’’ and ‘‘transversal’’ although the components  $A^{\parallel}$  and  $A^{\perp}$  have this property only for a vanishing background field  $a = 0$ .

is the total color charge density, which contains besides the external charge  $\rho_{\text{ext}}$  also the dynamical charge of the gauge bosons in the background gauge (33)

$$\rho_{\text{dyn}}[A] = -\hat{\mathbf{D}}\mathbf{\Pi}^\perp. \quad (54)$$

Rewriting the covariant derivative as

$$\hat{D} = \hat{d} + (\hat{A} - \hat{a}) \quad (55)$$

and using  $\hat{\mathbf{d}}\mathbf{\Pi}^\perp = 0$ , the dynamical charge becomes

$$\rho_{\text{dyn}}[A] = -(\hat{\mathbf{A}} - \hat{\mathbf{a}}) \mathbf{\Pi}^\perp. \quad (56)$$

It depends only on the fluctuation  $\mathcal{A} = A - a$  of the gauge field  $A$  around the background field  $a$ . Since the  $\hat{l}, \hat{t}$  (49) are orthogonal projectors we have

$$\mathbf{\Pi}^2 = \mathbf{\Pi}^{\parallel 2} + \mathbf{\Pi}^{\perp 2}. \quad (57)$$

Using this relation and Eq. (52) we find for the gauge fixed Yang–Mills Hamiltonian

$$H[A] = \frac{1}{2} \left( g^2 J^{-1}[A] \mathbf{\Pi}^\perp J[A] \mathbf{\Pi}^\perp + \frac{1}{g^2} \mathbf{B}[A^\perp] \mathbf{B}[A^\perp] \right) + H_C[A], \quad (58)$$

where

$$J[A] = \text{Det } \tilde{\mathcal{M}}[A] = \text{Det}(-\hat{\mathbf{D}}\hat{\mathbf{d}}) \quad (59)$$

is the Faddeev–Popov determinant (cf. Eq. (34)) and

$$H_C[A] = \frac{g^2}{2} J^{-1}[A] \rho(1) J[A] F[A](1, 2) \rho(2) \quad (60)$$

arises from the elimination of the longitudinal component of the momentum operator  $\mathbf{\Pi}^\parallel$  by means of Gauss’ law, see Eq. (52), and describes the interaction between the color charges. Here

$$F[A] = \left( -\hat{\mathbf{D}}\hat{\mathbf{d}} \right)^{-1} \left( -\hat{\mathbf{d}}\hat{\mathbf{d}} \right) \left( -\hat{\mathbf{D}}\hat{\mathbf{d}} \right)^{-1} \quad (61)$$

is the analogue of the so-called Coulomb kernel [6] in the background gauge (33). For a vanishing background field  $a = 0$  the covariant background derivative  $\hat{d} = \partial + \hat{a}$  becomes the  $\nabla$ -operator and the kernel (61) reduces to the ordinary Coulomb kernel [6].

In the gauge-fixed theory the matrix elements of an observable  $\mathcal{O}[\mathbf{\Pi}, A]$  are defined by

$$\langle \psi | \mathcal{O} | \phi \rangle = \int \mathcal{D}A \delta(\tilde{f}[A]) J[A] \psi^*[A] \mathcal{O}[\mathbf{\Pi}, A] \phi[A], \quad (62)$$

where  $\tilde{f}[A] = 0$  is the gauge fixing constraint (33) and  $J[A]$  (Eq. (59)) the corresponding Faddeev–Popov determinant (59).

### C. Choice of the wave functional

In Ref. [6] a variational determination of the Yang–Mills vacuum wave functional was carried out (in the absence of an external background field) in Coulomb gauge using the Gaussian type wave functional<sup>4</sup>

$$\begin{aligned} \psi_0[A] &= J^{-1/2}[A] \tilde{\psi}[A] \\ \tilde{\psi}[A] &:= \mathcal{N} \exp \left[ -\frac{1}{2g^2} A(1) \omega(1, 2) A(2) \right]. \end{aligned} \quad (63)$$

Here  $\mathcal{N}$  is a normalization constant and  $\omega$  is the variational kernel. The ansatz (63) has the advantage that it removes the Faddeev–Popov determinant  $J[A]$  from the integration measure (62). Here we extend the variational calculations to the presence of an external background field  $a$ . To fulfill the constraint  $\langle A \rangle_a = a$  we use the trial wave functional

$$\psi_a[A] = J^{-1/2}[A] \tilde{\psi}[A - a], \quad (64)$$

with  $\tilde{\psi}[A]$  defined in Eq. (63). In the absence of the background field  $\psi_a[A]$  reduces to the vacuum wave functional  $\psi_0[A]$  (63). This trial wave functional satisfies already the constraint (46), so it remains to minimize the energy  $\langle H \rangle_a$  with respect to the kernel  $\omega(1, 2)$ . Due to the presence of the colored background field the resulting kernel  $\omega(1, 2)$  will be a non-trivial matrix in color space.

With the trial wave functional (64) we find for the expectation value of any observable  $\mathcal{O}[\mathbf{\Pi}, A]$  from Eq. (62) after the shift<sup>5</sup>  $(A - a) \rightarrow A$  of integration variables

$$\begin{aligned} \langle \mathcal{O} \rangle_a &\equiv \langle \psi_a | \mathcal{O}[\mathbf{\Pi}, A] | \psi_a \rangle \\ &= \int \mathcal{D}A \delta(\tilde{f}[A + a]) \tilde{\psi}^*[A] \tilde{\mathcal{O}}[\mathbf{\Pi}, A + a] \tilde{\psi}[A] \\ &=: \langle \mathcal{O}[\mathbf{\Pi}, A + a] \rangle_0, \end{aligned} \quad (65)$$

where we have introduced the abbreviation

$$\tilde{\mathcal{O}}[\mathbf{\Pi}, A] = J^{1/2}[A] \mathcal{O}[\mathbf{\Pi}, A] J^{-1/2}[A]. \quad (66)$$

Equation (65) is the vacuum expectation value of the observable  $\tilde{\mathcal{O}}[\mathbf{\Pi}, A + a]$  in the gauge fixed theory with the gauge condition, Eq. (33)

$$\tilde{f}[A + a] = \hat{\mathbf{d}}\mathbf{A} = 0. \quad (67)$$

Note that in  $\langle \mathcal{O} \rangle_a$ , (65), the gauge constraint (67) is implemented, which eliminates the longitudinal gauge field  $A^\parallel$  defined by Eq. (51). Equation (65) applies in particular to the gauge fixed Hamiltonian (58). Note also that

<sup>4</sup> To be more precise in Ref. [6] the ansatz (63) was used with  $J[A]$  (59) replaced by the Faddeev–Popov determinant in Coulomb gauge  $\text{Det}(-\mathbf{D}\hat{\boldsymbol{\theta}})$ . Furthermore in the present case  $\omega(1, 2)$  can have a non-trivial color structure.

<sup>5</sup> Note that the momentum operator  $\mathbf{\Pi}$  remains unchanged under the shift of coordinates  $(A - a) \rightarrow A$ .

after the shift of variables  $(A - a) \rightarrow A$  the color charge of the gauge field (56) becomes

$$\rho_{\text{dyn}}[A + a] = -\hat{\mathbf{A}}\mathbf{\Pi}^\perp, \quad (68)$$

which is formally the same expression as obtained in Coulomb gauge [6, 34] except that transversality is now defined by the gauge condition (67) and thus depends on the background field  $a$ .

In passing we notice that in the gauge fixed Hamiltonian  $H[\mathbf{\Pi}, A]$  (58) the gauge field enters only in form of the covariant derivative  $\hat{D} = \partial + A$ . (Recall that the non-Abelian magnetic field can be written as  $B_i = \frac{1}{2}\epsilon_{ijk}[\hat{D}_j, \hat{D}_k]$ .) Therefore, after the shift of variables  $A \rightarrow A + a$  the Hamiltonian  $H[\mathbf{\Pi}, A + a]$  depends on the background field  $a$  only in the combination with the  $\nabla$ -operator  $\partial + \hat{a} = \hat{d}$ . This is, in particular, true for the Faddeev–Popov determinant (34)

$$J[A + a] = \text{Det} \left( - \left( \hat{d} + \hat{\mathbf{A}} \right) \hat{d} \right) \quad (69)$$

and thus also for the transformed Hamiltonian  $\tilde{H}[\mathbf{\Pi}, A + a]$  defined by Eq. (66).

We are eventually interested in the effective potential of the order parameter of confinement. For this purpose it is sufficient to consider constant background fields  $\mathbf{a}$ , which we will assume from now on. Note, since  $\hat{\mathbf{a}} \cdot \mathbf{a} = 0$ , for constant background fields  $\mathbf{a}$  we have  $\hat{\mathbf{d}} \cdot \mathbf{a} = 0$  and the gauge condition (33) reduces to the condition (67)  $\hat{\mathbf{d}} \cdot \mathbf{A} = 0$ . For the time being the color structure of the background field  $\hat{a} = a^b(\mathbf{x})\hat{T}_b$  is arbitrary.

## V. YANG–MILLS DYNAMICS IN THE PRESENCE OF A BACKGROUND FIELD

The presence of the background field influences the form of the propagators. In addition, the propagators depend on the gauge chosen. In the following we present the equation of motion for the ghost and gluon propagators following from the constrained variational principle (47) in the background gauge (67) with the trial wave functional (64). Thereby we will make no assumption on the form of background field (except that it is constant). The resulting equations of motion are direct generalizations of the equations obtained in the variational approach in Coulomb gauge [6] and reduce to the latter for a vanishing background field.

### A. The gluon propagator

Since by Eq. (65) all expectation values  $\langle \dots \rangle_a$  in the state  $|\psi_a\rangle$ , satisfying the constraint (46), can be reduced to the vacuum expectation value  $\langle \dots \rangle_0$  it suffices to consider the gluon propagator

$$\mathcal{D}(1, 2) = \langle A(1)A(2) \rangle_0, \quad (70)$$

which for the trial wave functional (63) is given by

$$\mathcal{D}(1, 2) = \frac{g^2}{2}\omega^{-1}(1, 2). \quad (71)$$

Independent of the form of the background field from the definition (70) follows the symmetry relation  $\mathcal{D}(1, 2) = \mathcal{D}(2, 1)$ , i.e.

$$\mathcal{D}_{kl}^{ab}(\mathbf{x}, \mathbf{y}) = \mathcal{D}_{lk}^{ba}(\mathbf{y}, \mathbf{x}). \quad (72)$$

Since the gauge field is “transverse” (w.r.t. the covariant background derivative  $d$  (50))

$$A_k^a(\mathbf{x}) = t_{kl}^{ab}(\mathbf{x})A_l^b(\mathbf{x}) \quad (73)$$

the gluon propagator is also “transverse” satisfying

$$t_{kk'}^{aa'}(\mathbf{x})t_{ll'}^{bb'}(\mathbf{y})\mathcal{D}_{k'l'}^{a'b'}(\mathbf{x}, \mathbf{y}) = \mathcal{D}_{kl}^{ab}(\mathbf{x}, \mathbf{y}). \quad (74)$$

Note, the ordering is here important since  $t(\mathbf{x})$  is a differential operator. By Wick’s theorem expectation values in the state  $\psi_0[A]$  (63) can be entirely expressed in terms of the gluon propagator (70), see Sect. VD.

### B. The ghost DSE

In the presence of the external background field the ghost propagator is defined by

$$G = \langle \tilde{\mathcal{M}}^{-1}[A] \rangle_a, \quad (75)$$

where  $\tilde{\mathcal{M}}[A]$  is the Faddeev–Popov kernel (34) and  $\langle \dots \rangle_a$  is defined in Eq. (65), from which follows that the ghost propagator can be expressed as vacuum expectation value

$$G = \left\langle \tilde{\mathcal{M}}^{-1}[A + a] \right\rangle_0 = \left\langle \left( - \left( \hat{d} + \hat{\mathbf{A}} \right) \hat{d} \right)^{-1} \right\rangle_0. \quad (76)$$

In the way described in Ref. [6] one derives for this ghost propagator the following Dyson–Schwinger equation

$$G^{-1} = G_0^{-1} - \Sigma, \quad (77)$$

where  $G_0$  is the bare ghost propagator, which is defined by Eq. (76) with  $A = 0$

$$G_0 = \left( -\hat{\mathbf{d}}\hat{\mathbf{d}} \right)^{-1}. \quad (78)$$

Furthermore, the ghost self-energy is given by

$$\Sigma(1, 2) = \Gamma_0(1, 3; 4)G(3, 3')\Gamma(3', 2; 4')\mathcal{D}(4', 4), \quad (79)$$

where  $\mathcal{D}(1, 2)$  is the gluon propagator (70) and

$$\Gamma_0(1, 2; 3) = \frac{\delta \tilde{\mathcal{M}}[A + a](1, 2)}{\delta A(3)} \quad (80)$$

is the bare ghost-gluon vertex. The full ghost-gluon vertex  $\Gamma$  is defined here by

$$\left\langle \tilde{\mathcal{M}}^{-1}[A + a]\Gamma_0\tilde{\mathcal{M}}^{-1}[A + a] \right\rangle_0 = G\Gamma G. \quad (81)$$

Following Ref. [6] we use the rainbow ladder approximation replacing the full ghost-gluon vertex by the bare one. The justification for this is the following: As shown in Landau gauge [35] the ghost-gluon vertex is not renormalized. This holds also in Coulomb gauge [10]. Furthermore, in Coulomb gauge the dressing of the ghost-gluon vertex, at least to one-loop order, is small [14]. We assume that this remains valid for the present gauge (67), which reduces to Coulomb gauge in the absence of the background field.

With the explicit form of the Faddeev–Popov kernel  $\tilde{\mathcal{M}}[A]$  (34) we find for the bare ghost-gluon vertex (80)

$$\begin{aligned} \Gamma_{0,k}^a(\mathbf{x}_1, \mathbf{x}_2; \mathbf{x}_3) \\ = \left( \hat{T}_b t_{lk}^{ba}(\mathbf{x}_1) \delta(\mathbf{x}_1 - \mathbf{x}_3) \right) \hat{d}_l(\mathbf{x}_1) \delta(\mathbf{x}_1 - \mathbf{x}_2), \end{aligned} \quad (82)$$

with  $\hat{T}_b^{ac} = f^{abc}$ . Here we have suppressed the adjoint color indices  $a_1, a_2$ , of the ghost legs and set

$$\Gamma(1, 2; 3) \equiv (\Gamma_{a_3 k_3}(\mathbf{x}_1, \mathbf{x}_2; \mathbf{x}_3))^{a_1 a_2}. \quad (83)$$

Replacing the full ghost-gluon vertex  $\Gamma$  by the bare one (82) we find for the ghost self-energy (79)

$$\begin{aligned} \Sigma(\mathbf{x}_1, \mathbf{x}_2) = & \left[ t_{kk'}^{aa'}(\mathbf{x}_1) t_{ll'}^{bb'}(\mathbf{x}_3) D_{l'k'}^{b'a'}(\mathbf{x}_3, \mathbf{x}_1) \right] \\ & \times \hat{T}_a \left( \hat{d}_k(\mathbf{x}_1) G(\mathbf{x}_1, \mathbf{x}_3) \right) \hat{T}_b \left( \hat{d}_l(\mathbf{x}_3) \delta(\mathbf{x}_3, \mathbf{x}_2) \right), \end{aligned} \quad (84)$$

which is still a matrix in adjoint color space.

### C. The curvature

The kinetic part of the transformed Yang–Mills Hamiltonian  $\tilde{H}$  cf. (66) contains functional derivatives of the Faddeev–Popov determinant. In the vacuum expectation value of  $\tilde{H}$  (see subsection VD) these derivatives enter in form of the ghost loop

$$\chi(1, 2) = -\frac{1}{2} \left\langle \frac{\delta^2 \ln J[A+a]}{\delta A(1) \delta A(2)} \right\rangle_0, \quad (85)$$

which in the present context is referred to as curvature [6]. The curvature is defined here as in Ref. [6], however, with the argument of the Faddeev–Popov determinant shifted by the background field. With the definition of the ghost-gluon vertex (81) it can be expressed as (cf. Ref. [6] for more details)

$$\chi(1, 2) = \frac{1}{2} \text{Tr} (G\Gamma(1)G\Gamma_0(2)). \quad (86)$$

Using again the bare ghost-gluon vertex approximation one finds with (82)

$$\begin{aligned} \chi_{kl}^{ab}(\mathbf{y}_1, \mathbf{y}_2) = & \frac{1}{2} t_{kk'}^{aa'}(\mathbf{y}_1) t_{ll'}^{bb'}(\mathbf{y}_2) \\ & \times \text{tr} \left[ \hat{T}_{a'} \left( \hat{d}_{k'}(\mathbf{y}_1) G(\mathbf{y}_1, \mathbf{y}_2) \right) \hat{T}_b \hat{d}_{l'}(\mathbf{y}_2) G(\mathbf{y}_2, \mathbf{y}_1) \right], \end{aligned} \quad (87)$$

where the trace is over the adjoint color space.

### D. The energy density and the gap equation

Since the vacuum wave functional  $\tilde{\psi}[A]$  (63) is Gaussian it is straightforward to calculate the energy  $\langle H \rangle_a$  (cf. (65)) by using Wick's theorem and expressing  $\langle H[\Pi, A+a] \rangle_0$  as a functional of the gluon propagator  $\mathcal{D}$  (70). For the Abelian part of the magnetic energy one finds

$$\langle H_B^A \rangle_a = \frac{1}{2g^2} \left[ (-\hat{\mathbf{d}}\hat{\mathbf{d}})(1, 2) \mathcal{D}(2, 1') \right]_{1'=1} \quad (88)$$

while the non-Abelian part gives

$$\begin{aligned} \langle H_B^{NA} \rangle_a = & \frac{1}{4g^2} f^{abc} f^{ab'c'} \int d^d x \left[ \mathcal{D}_{ll'}^{bb'}(x, x) \mathcal{D}_{mm}^{cc'}(x, x) \right. \\ & \left. + \mathcal{D}_{lm}^{bc}(x, x) \mathcal{D}_{lm}^{b'c'}(x, x) + \mathcal{D}_{lm}^{bc'}(x, x) \mathcal{D}_{lm}^{b'c}(x, x) \right]. \end{aligned} \quad (89)$$

For the expectation value of the kinetic part  $\tilde{H}_K$  of the transformed Hamiltonian (66)

$$\begin{aligned} \tilde{H}_K[A] = & \frac{g^2}{2} \left\{ \Pi(1)\Pi(1) + \frac{1}{2} \left( \frac{\delta}{\delta A(1)} \frac{\delta}{\delta A(1)} \ln J[A] \right) \right. \\ & \left. + \frac{1}{4} \frac{\delta \ln J[A]}{\delta A(1)} \frac{\delta \ln J[A]}{\delta A(1)} \right\} \end{aligned} \quad (90)$$

one finds, using the definition of the curvature (85) (see Refs. [6, 17] for more details)

$$\begin{aligned} \langle H_K \rangle_a = & \frac{g^2}{2} \left\{ \frac{\mathcal{D}^{-1}(1, 1)}{4} - \chi(1, 1) + \chi(1, 2) \mathcal{D}(2, 3) \chi(3, 1) \right\}. \end{aligned} \quad (91)$$

Variation of the energy  $\langle H \rangle_a$  with respect to the gluon propagator  $\mathcal{D}$  (70) yields the gap equation. As shown in Ref. [17] the Coulomb term  $H_C$  has little influence on the gluon sector. Furthermore, the non-Abelian part of the magnetic energy gives rise to a tadpole, which in the absence of the background field contributes a (UV-diverging) constant to the gap equation, which can be absorbed into a renormalization constant. Ignoring the Coulomb term and the non-Abelian part of the magnetic energy the gap equation arising from

$$\langle H_K + H_B^A \rangle_a \rightarrow \min \quad (92)$$

becomes

$$\frac{g^4}{4} \mathcal{D}^{-1}(2, 3) \mathcal{D}^{-1}(3, 1) = (-\hat{t}\hat{\mathbf{d}}\hat{t})(2, 1) + g^4 \chi(2, 3) \chi(3, 1). \quad (93)$$

Here we have also ignored the derivatives  $\delta\chi/\delta\mathcal{D}$ , which give rise to two-loop terms since  $\chi$  itself contains already one ghost loop. Using the gap equation (93) to express  $(-\hat{t}\hat{\mathbf{d}})$  in the magnetic energy in terms of  $\mathcal{D}$  and  $\chi$  the vacuum energy can be cast into the compact form

$$\langle H_K + H_B^A \rangle_a = g^2 \left[ \frac{1}{2} \mathcal{D}^{-1}(1, 1) - \chi(1, 1) \right]. \quad (94)$$

In Sect. VIII we will extract from this expression the effective potential of the order parameter of confinement.

## VI. THE PROPAGATORS IN THE PRESENCE OF THE BACKGROUND FIELD

The above considerations are valid for any gauge group and for arbitrary constant background fields. For pedagogical reason we will confine ourselves below to the gauge group SU(2). The extension to SU( $N$ ) is straightforward and will be presented in Subsect. VID.

### A. Choice of the background field

As shown in Sect. II to find the effective potential of the confinement order parameter, it is sufficient to consider constant background fields  $\mathbf{a} = \text{const}$ . By isotropy of space, without loss of generality we can direct the background field along the 3-axis

$$\mathbf{a} = a\mathbf{e}_3. \quad (95)$$

Furthermore, as we have seen in Sect. II the background field has to live in the Cartan subalgebra to figure as order parameter of confinement. Therefore we have to choose for SU(2)

$$a \equiv a^b T_b = a T_3, \quad a = \text{const}. \quad (96)$$

In the Hamiltonian approach presented above the background field occurs in the adjoint representation. The Cartan generator in the adjoint representation  $\hat{T}_3 = \epsilon^{a3b}$  is diagonalized in the basis of the spin  $s = 1$  eigenstates

$$\hat{T}_3|\sigma\rangle = -i\sigma|\sigma\rangle, \quad \sigma = 0, \pm 1, \quad (97)$$

where, in the usual bracket notation, the

$$\langle a|\sigma\rangle = e_\sigma^a \quad (98)$$

are the cartesian components of the spherical unit vectors (in color space)

$$\mathbf{e}_{\sigma=1} = -\frac{1}{\sqrt{2}} \begin{pmatrix} 1 \\ i \\ 0 \end{pmatrix}, \quad \mathbf{e}_{\sigma=-1} = \frac{1}{\sqrt{2}} \begin{pmatrix} 1 \\ -i \\ 0 \end{pmatrix}, \quad \mathbf{e}_{\sigma=0} = \begin{pmatrix} 0 \\ 0 \\ 1 \end{pmatrix}. \quad (99)$$

Here and in the following Greek letters  $\sigma, \tau, \rho, \dots$  denote spherical color components (1, 0, -1) while Latin letters  $a, b, c, \dots$  denote the Cartesian color components (1, 2, 3). The vectors  $\mathbf{e}_\sigma$  satisfy the symmetry relation

$$\mathbf{e}_\sigma^* = (-)^\sigma \mathbf{e}_{-\sigma} \quad (100)$$

and form an orthonormal 3-bein

$$\mathbf{e}_\sigma^* \mathbf{e}_\tau = \delta_{\sigma\tau}, \quad \mathbf{e}_\rho \times \mathbf{e}_\sigma = -i\epsilon_{\rho\sigma\tau} \mathbf{e}_\tau^*. \quad (101)$$

By Eq. (97) we have

$$\hat{a}|\sigma\rangle = a\hat{T}_3|\sigma\rangle = -ia\sigma|\sigma\rangle. \quad (102)$$

Any matrix in the adjoint representation can be expressed in the spherical basis as

$$M^{ab} = \sum_{\sigma, \tau} \langle a|\sigma\rangle M^{\sigma\tau} \langle \tau|b\rangle. \quad (103)$$

Due to Eq. (102), the covariant derivative (50)  $\hat{d}_k$  becomes diagonal in the spherical basis

$$d_k^{\sigma\tau} = \delta^{\sigma\tau} d_k^\sigma, \quad d_k^\sigma = \partial_k + \delta_{k3}(-i\sigma a). \quad (104)$$

The same is true for the longitudinal and transversal projectors (49)

$$\begin{aligned} l_{kl}^{\sigma\tau} &= \delta^{\sigma\tau} l_{kl}^\sigma, & l_{kl}^\sigma &= d_k^\sigma (\mathbf{d}^\sigma \mathbf{d}^\sigma)^{-1} d_l^\sigma \\ t_{kl}^{\sigma\tau} &= \delta^{\sigma\tau} t_{kl}^\sigma, & t_{kl}^\sigma &= \delta_{kl} - l_{kl}^\sigma, \end{aligned} \quad (105)$$

which makes the spherical basis favorable. Defining the momentum representation of these quantities by

$$\begin{aligned} d(x)e^{i\mathbf{p}\mathbf{x}} &= d(\mathbf{p})e^{i\mathbf{p}\mathbf{x}} \\ t(x)e^{i\mathbf{p}\mathbf{x}} &= t(\mathbf{p})e^{i\mathbf{p}\mathbf{x}} \end{aligned} \quad (106)$$

we have in the spherical basis

$$d_k^\sigma(\mathbf{p}) = i(\mathbf{p} - \sigma a \mathbf{e}_3)_k = i(p_k - \sigma a \delta_{k3}), \quad (107)$$

$$t_{kl}^\sigma(\mathbf{p}) = \delta_{kl} - \frac{d_k^\sigma(\mathbf{p})d_l^\sigma(\mathbf{p})}{\mathbf{d}^\sigma(\mathbf{p})\mathbf{d}^\sigma(\mathbf{p})}, \quad (108)$$

where

$$-\mathbf{d}^\sigma(\mathbf{p})\mathbf{d}^\sigma(\mathbf{p}) = (\mathbf{p} - \sigma a \mathbf{e}_3)^2 = \mathbf{p}_\perp^2 + (p_3 - \sigma a)^2 \quad (109)$$

and  $\mathbf{p}_\perp$  is the projection of  $\mathbf{p}$  on the 1-2-plane. Furthermore these quantities satisfy the symmetry relations

$$\begin{aligned} t_{kl}^\sigma(\mathbf{p}) &= t_{lk}^\sigma(\mathbf{p}), & t_{kl}^\sigma(-\mathbf{p}) &= t_{kl}^{-\sigma}(\mathbf{p}), \\ d_k^\sigma(-\mathbf{p}) &= -d_k^{-\sigma}(\mathbf{p}). \end{aligned} \quad (110)$$

### B. Propagators

For a constant background field the homogeneity of space is preserved and the Green's functions can depend only on coordinate differences and thus can be Fourier transformed as in the absence of the background field. We define the Fourier transform for the gluon propagator by

$$\mathcal{D}(\mathbf{x}, \mathbf{y}) = \int d\mathbf{p} e^{i\mathbf{p}(\mathbf{x}-\mathbf{y})} \mathcal{D}(\mathbf{p}), \quad d\mathbf{p} \equiv \frac{d\mathbf{p}}{(2\pi)^d} \quad (111)$$

and analogously for the other two-point functions like ghost propagator and curvature. The background field (96), however, singles out a direction in 3-space and thus

spoils SO(3) invariance. Therefore the Fourier transformed two-point functions, like  $\mathcal{D}(\mathbf{p})$ , will not just depend on the modulus  $|\mathbf{p}|$  but also on the direction of  $\mathbf{p}$ .

Since the background field  $\hat{a} = a\hat{T}_3$  is diagonal in the spherical basis and since  $\hat{a}$  is the only color dependent quantity we expect that the various two-point functions like gluon and ghost propagators are also diagonal in this basis. We show in appendix A that the equations of motion can indeed be consistently solved for color diagonal propagators of the form

$$\mathcal{D}_{kl}^{\sigma\tau}(\mathbf{p}) = \delta^{\sigma\tau} t_{kl}^\sigma(\mathbf{p}) \mathcal{D}^\sigma(\mathbf{p}) \quad (112)$$

$$G^{\sigma\tau}(\mathbf{p}) = \delta^{\sigma\tau} G^\sigma(\mathbf{p}). \quad (113)$$

For the reduced propagators  $G^\sigma(p)$ ,  $\mathcal{D}^\sigma(p)$  the equations of motion simplify drastically. From the appendix A we find for the ghost DSE (A21)

$$G^\sigma(\mathbf{p})^{-1} = G_0^\sigma(\mathbf{p})^{-1} - \Sigma^\sigma(\mathbf{p}), \quad (114)$$

where

$$G_0^\sigma(\mathbf{p})^{-1} = -\mathbf{d}^\sigma(\mathbf{p})\mathbf{d}^\sigma(\mathbf{p}) = (\mathbf{p} - \mathbf{e}_3\sigma a)^2 \quad (115)$$

is the bare (inverse) ghost propagator (78) and

$$\begin{aligned} \Sigma^\sigma(\mathbf{p}) = & \\ - \sum_\mu \int \bar{\mathbf{d}}q \, d_l^\sigma(\mathbf{p}) t_{lk}^\mu(\mathbf{q}) d_k^\sigma(\mathbf{p}) \mathcal{D}^\mu(\mathbf{q}) G^{\sigma+\mu}(\mathbf{p} + \mathbf{q}) & \quad (116) \end{aligned}$$

is the ghost self-energy (84). Here and in the following sums of spherical indices, like  $\mu + \sigma$ , are defined modulo 3. As shown in the appendix A we find for the gap equation (A33) after the transversal projectors are contracted

$$\frac{g^4}{4} (\mathcal{D}^\sigma(\mathbf{p}))^{-2} = -\mathbf{d}^\sigma(\mathbf{p})\mathbf{d}^\sigma(\mathbf{p}) + g^4 (\chi^\sigma(\mathbf{p}))^2, \quad (117)$$

where (cf. Eq. (A31))

$$\begin{aligned} \chi^\sigma(\mathbf{p}) = & -\frac{g^2}{2(d-1)} \\ \times \sum_\mu \int \bar{\mathbf{d}}q \, d_k^\mu(\mathbf{q}) g_{kl}^\sigma(\mathbf{p}) d_l^\mu(\mathbf{q}) G^\mu(\mathbf{q}) G^{\sigma+\mu}(\mathbf{p} + \mathbf{q}) & \quad (118) \end{aligned}$$

is the scalar curvature. Finally from Eq. (A35) we have for the energy (94)

$$\begin{aligned} \langle H_K + H_B^A \rangle_a = & \\ (d-1)V \sum_\sigma \int \bar{\mathbf{d}}q \left( \frac{g^2}{2} \mathcal{D}^\sigma(\mathbf{q})^{-1} - \chi^\sigma(\mathbf{q}) \right) & \quad (119) \end{aligned}$$

Let us emphasize that  $G^\sigma(\mathbf{p})$ ,  $\Sigma^\sigma(\mathbf{p})$ ,  $\mathcal{D}^\sigma(\mathbf{p})$  and  $\chi^\sigma(\mathbf{p})$  are all scalars in  $\mathbb{R}^3$  but have a non-trivial color structure due to their dependence on the spherical color index  $\sigma$ .

### C. Relating the propagators in the presence of the background field to the vacuum propagators in Coulomb gauge

The solutions of the constraint variational problem (47) are defined by the coupled equations (114), (117), in which the expressions (116)  $\Sigma^\sigma(\mathbf{p})$  and (118)  $\chi^\sigma(\mathbf{p})$  enter. It is not difficult to see that solutions exist, which obey the symmetry relations

$$\mathcal{D}^\mu(-\mathbf{p}) = \mathcal{D}^{-\mu}(\mathbf{p}), \quad G^\mu(-\mathbf{p}) = G^{-\mu}(\mathbf{p}). \quad (120)$$

Indeed assuming that these relations hold, one finds from the explicit expressions for  $\Sigma$  (116) and  $\chi$  (118) by using (110)

$$\Sigma^\mu(-\mathbf{p}) = \Sigma^{-\mu}(\mathbf{p}), \quad \chi^\mu(-\mathbf{p}) = \chi^{-\mu}(\mathbf{p}), \quad (121)$$

which in turn entails Eqs. (120). We will now show that these solutions can be related to the vacuum solution in Coulomb gauge obtained in Ref. [6].

Fourier transforming Eq. (71), going to the spherical basis (103) and assuming (112) we have

$$\mathcal{D}^\sigma(\mathbf{p}) = \frac{g^2}{2\omega^\sigma(\mathbf{p})}, \quad (122)$$

where  $\omega^\sigma(\mathbf{p})$  is the energy of a gluon with spherical color component  $\sigma$ . Using also Eqs. (115) and Eq. (A28) from appendix A the gap equation (117) becomes

$$(\omega^\sigma(\mathbf{p}))^2 = (\mathbf{p} - \sigma a \mathbf{e}_3)^2 + (\chi^\sigma(\mathbf{p}))^2, \quad (123)$$

which is now a scalar equation. It differs from the vacuum gap equation in Coulomb gauge obtained in Ref. [6] by the explicit presence of background field  $a$  in the first term of the r.h.s.<sup>6</sup> and by the index  $\sigma$  labeling the eigenvalues of  $-i\hat{T}_3$ . Obviously, the gap equation (123) allows for solution of the form

$$\omega^\sigma(\mathbf{p}) = \omega(\mathbf{p}_\sigma), \quad (124)$$

where

$$\mathbf{p}_\sigma := \mathbf{p} - \sigma a \mathbf{e}_3 \quad (125)$$

and  $\omega(\mathbf{p})$  is the solution in the absence of the background field, i.e. for  $a = 0$ , provided also the curvature has the property:

$$\chi^\sigma(\mathbf{p}) = \chi(\mathbf{p}_\sigma). \quad (126)$$

We will now explicitly show that both the gap equation (123) and the ghost DSE (114) are indeed satisfied by propagators of the form

$$\mathcal{D}^\sigma(\mathbf{p}) = \mathcal{D}(\mathbf{p}_\sigma), \quad G^\sigma(\mathbf{p}) = G(\mathbf{p}_\sigma), \quad (127)$$

<sup>6</sup> As, compared to Ref. [6], in the present paper we have ignored the tadpole and the Coulomb term.

where  $\mathcal{D}(\mathbf{p})$  and  $G(\mathbf{p})$  are the corresponding propagators for  $a = 0$ , i.e. the vacuum solutions of the Hamiltonian approach in Coulomb gauge [6].

First notice that by the definitions (107), (108) we have

$$d^\sigma(\mathbf{p}) = d(\mathbf{p}_\sigma), \quad t^\sigma(\mathbf{p}) = t(\mathbf{p}_\sigma). \quad (128)$$

Assuming (127) and noticing that by Eq. (125)

$$(\mathbf{p} + \mathbf{q})_{\sigma+\mu} = \mathbf{p}_\sigma + \mathbf{q}_\mu \quad (129)$$

from Eq. (116) follows indeed with (128)

$$\Sigma^\sigma(\mathbf{p}) = \Sigma(\mathbf{p}_\sigma) \quad (130)$$

and thus the ghost DSE (114) allows indeed for solutions of the form (127). In the same way one shows that, assuming (127), from Eq. (118) follows

$$\chi^\sigma(\mathbf{p}) = \chi(\mathbf{p}_\sigma), \quad (131)$$

which implies that also the gap equation (123) allows for solutions of the form (127). This completes the proof of existence of solutions of the form (127). Since the propagators in the absence of the background field depend only on  $\mathbf{p}^2$  the solutions (127) also satisfy the symmetry relation (120). We have thus shown that the propagators in the background gauge (67) in the state of minimal energy under the constraint (46) are related by Eq. (127) to the ordinary vacuum propagators in Coulomb gauge<sup>7</sup>. The latter have been determined previously in a variational approach in the continuum theory [6, 9] as well as measured on the lattice [36]. In the section VIII, we will use these propagators as input to calculate the effective potential of the confinement order parameter. For this purpose we briefly review in Sect. VII the results obtained for  $\omega(\mathbf{p})$  and  $\chi(\mathbf{p})$  in the Hamiltonian approach in Coulomb gauge at zero temperature.

#### D. Extension to $SU(N)$

The previous considerations can be straightforwardly extended to an arbitrary gauge group  $SU(N)$ . As explained in Sect. II the background field  $a$  has to be chosen in the Cartan subalgebra

$$a = \sum_{k=1}^r a^k H_k, \quad (132)$$

where

$$H_k, \quad k = 1, \dots, r \quad (133)$$

are the generators of the Cartan subalgebra with  $r$  being the rank of the group. Since the  $H_k$  commute with each other they can be simultaneously diagonalized. Their eigenvalues are the so-called weights  $-i\mu_k$ , which are the entries of the weight vectors

$$\boldsymbol{\mu} = (\mu_1, \dots, \mu_r). \quad (134)$$

In the present approach we need the background field in the adjoint representation  $\hat{a}$ . The weights in the adjoint representation  $\hat{H}_k$  are the roots  $\sigma_k$

$$\hat{H}_k|\sigma\rangle = -i\sigma_k|\sigma\rangle, \quad (135)$$

which are the entries of the root vectors

$$\boldsymbol{\sigma} = (\sigma_1, \dots, \sigma_r). \quad (136)$$

For the gauge group  $SU(2)$ , which has rank  $r = 1$ , the single generator of the Cartan subalgebra is given by  $H_1 = T_3$  and the eigenbasis of  $\hat{T}_3$  is explicitly given in Eq. (99). As in the  $SU(2)$  case, in the Cartan basis (135) the background field (132) is obviously diagonal

$$\hat{a}|\sigma\rangle = -i\mathbf{a}\boldsymbol{\sigma}|\sigma\rangle, \quad (137)$$

where  $\mathbf{a} = (a_1, \dots, a_r)$  and

$$\mathbf{a}\boldsymbol{\sigma} = \sum_{k=1}^r a_k \sigma_k \quad (138)$$

is the scalar product in the Cartan subalgebra. Furthermore for  $SU(N)$  the non-vanishing roots come in pairs  $\pm\boldsymbol{\sigma}$ . (Some of the roots may vanish as in the  $SU(2)$  case. In the mathematical literature the term “root” is usually reserved to the non-vanishing roots.) Besides  $SU(2)$ , we will be mainly interested in the gauge group  $SU(3)$ , which has rank 2. The two generators of the Cartan subalgebra are usually chosen as  $H_1 = T_3$  and  $H_2 = T_8$ . For this group the positive weights read

$$\boldsymbol{\mu} = \left(0, \frac{1}{\sqrt{3}}\right), \quad \left(\frac{1}{2}, \frac{1}{2\sqrt{3}}\right), \quad \left(\frac{1}{2}, -\frac{1}{2\sqrt{3}}\right) \quad (139)$$

and the non-vanishing positive<sup>8</sup> roots are given by

$$\boldsymbol{\sigma} = (1, 0), \quad \left(\frac{1}{2}, \frac{1}{2}\sqrt{3}\right), \quad \left(\frac{1}{2}, -\frac{1}{2}\sqrt{3}\right), \quad (140)$$

where the first root occurs also in the  $SU(2)$  case. Note that for  $SU(3)$  the scalar product of a root vector with a weight vector is either 0 or  $\frac{1}{2}$

$$\boldsymbol{\sigma}\boldsymbol{\mu} \in \{0, \frac{1}{2}\}. \quad (141)$$

<sup>7</sup> In principle, there could, of course, be other solutions which do not have the form (127). So far we have no indication that such solutions do exist.

<sup>8</sup> A weight or a root is called “positive” if its first component is positive.

All considerations of the previous section remain valid for SU(3) with the only modification that the shifted momentum (125) has to be replaced by

$$\mathbf{p}_\sigma = \mathbf{p} - (\boldsymbol{\sigma}\mathbf{a})\mathbf{e}_3, \quad (142)$$

where  $\boldsymbol{\sigma}\mathbf{a}$  is defined in Eq. (138). With this modification all equations of the previous section remain valid when the index  $\sigma = 0, \pm 1$  is replaced in SU(3) by all (2-dimensional) root vectors  $\boldsymbol{\sigma}$ . Since the roots (140) are normalized  $\boldsymbol{\sigma}\boldsymbol{\sigma} = 1$  the co-weight vectors  $\tilde{\mu}_k$  (Eq. (2)) are given by  $2\boldsymbol{\mu}$  and accordingly the non-trivial center elements read

$$e^{-4\pi\boldsymbol{\mu}\mathbf{H}} = z, \quad (143)$$

where  $H_1 = T_3, H_2 = T_8$  are the generators of the Cartan algebra in the fundamental representation, normalized to  $\text{tr}(T_a T_b) = -\frac{1}{2}\delta_{ab}$ . Center symmetry of the effective potential (9) requires that it remains invariant under the replacement of the background field

$$\mathbf{a} \rightarrow \mathbf{a} + \frac{4\pi}{L}\boldsymbol{\mu}, \quad (144)$$

where  $\boldsymbol{\mu}$  represents one of the roots (139).

## VII. THE COULOMB GAUGE PROPAGATORS

Since  $\mathbf{p}_{\sigma=0} = \mathbf{p}$  (see Eq. (125)) by Eq. (127) the zero-temperature propagators in Coulomb gauge (for vanishing background field) are given by the background gauge propagators with  $\sigma = 0$ . Putting  $\sigma = 0$  in Eq. (123) the zero-temperature gap equation in Coulomb gauge becomes in the presently used approximation

$$\omega^2(\mathbf{p}) = \mathbf{p}^2 + \chi^2(\mathbf{p}). \quad (145)$$

Since  $\chi(\mathbf{p}) = \chi^{\sigma=0}(\mathbf{p})$  (118) is defined in terms of the ghost propagator  $G^\sigma(\mathbf{p})$  this equation has to be solved simultaneously with the ghost DSE (114). Introducing the ghost form factor  $d(\mathbf{p})$  by

$$G^{\sigma=0}(\mathbf{p}) = \frac{d(\mathbf{p})}{g\mathbf{p}^2} \quad (146)$$

the ghost DSE becomes

$$d^{-1}(\mathbf{p}) = \frac{1}{g} + I_d(\mathbf{p}), \quad (147)$$

$$I_d(\mathbf{p}) = N_c \int \tilde{d}q [1 - (\hat{\mathbf{p}}\hat{\mathbf{q}})^2] \frac{d(\mathbf{p}-\mathbf{q})}{(\mathbf{p}-\mathbf{q})^2} \frac{1}{2\omega(\mathbf{q})}.$$

Equations (145) and (147) can be solved analytically in the IR using the power law ansätze [6, 10, 17]

$$\omega(p) = \frac{A}{p^\alpha}, \quad d(p) = \frac{B}{p^\beta}, \quad (148)$$

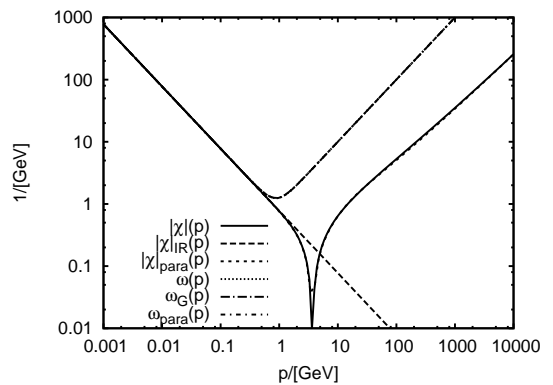


FIG. 1. The gluon energy  $\omega(p)$  and modulus of the curvature  $\chi(p)$  resulting from the full numerical solution of the variational approach in Coulomb gauge as described in Ref. [17]. The Figure contains also the Gribov formula (151) fitted to the numerical data for  $\omega(p)$ , as well as the IR form  $\chi_{\text{IR}}$  (152) of the curvature. In addition we also show the parameterization (154)  $\chi_{\text{para}}(p)$  to the numerical results for  $\chi(p)$ , together with the solution  $\omega_{\text{para}}(p)$  of the gap equation (145) assuming the optimal parameterization  $\chi_{\text{para}}(p)$  (154) as input.

with  $p = |\mathbf{p}|$ . From the ghost DSE (147) one finds the sum rule

$$\alpha = 2\beta - d + 2 \quad (149)$$

For  $d = 3$  the gap equation (145) allows then for two solutions with ghost IR exponents

$$\beta = 1, \quad \beta = 0.795. \quad (150)$$

The first one, for which  $\alpha = 1$ , is compatible with the gluon propagator measured on the lattice. Indeed, the lattice results [36] for the gluon energy  $\omega(p)$  can be well fitted by the Gribov formula [37]

$$\omega_G(p) = \sqrt{p^2 + \frac{M^4}{p^2}} \quad (151)$$

with a mass  $M \simeq 880$  MeV for SU(2) [36] and about the same value for SU(3) [38]. Using for  $\omega(p)$  the Gribov formula (151) we find from the gap equation (145) for the curvature

$$\chi(p) = \frac{M^2}{p} =: \chi_{\text{IR}}(p), \quad (152)$$

which represents the correct infrared behavior of  $\chi(p)$  obtained in Refs. [6, 10, 11]. What is missing in the expression (152) is the UV-part

$$\chi_{\text{UV}}(p) = c \frac{\sqrt{p^2 + \lambda}}{\ln \frac{p^2 + \lambda}{M^2}} \xrightarrow{p \rightarrow \infty} c \frac{p}{\ln \frac{p^2}{M^2}}, \quad c = \text{const}, \quad (153)$$

which arises in a self-consistent solution of the coupled ghost DSE (147) and gap equation (145) [6],[17]. In the

gap equation (145) this term is UV-subleading compared to the UV-leading term  $\omega(p) \sim p$ .

Alternative to the use of the lattice result we solve the ghost DSE (147) and the gap equation (145) numerically in the way described in Ref. [17], where also the renormalization of these equations is discussed in detail. The resulting numerical solutions for  $\omega(p) = \omega^{\sigma=0}(p)$  and  $\chi(p) = \chi^{\sigma=0}(p)$  are shown in Fig. 1 for the  $\beta = 1$  solution. The physical scale is determined as in Ref. [17] by fitting the numerical results for  $\omega(p)$  to the Gribov formula (151), using the lattice result of  $M = 880$  MeV as input. Fig. 1 shows also the fit of the the Gribov formula (151) to the numerical results for  $\omega(p)$  and  $\chi_{\text{IR}}(p)$  (152). In the double logarithmic plot the Gribov formula (151) is indistinguishable from the numerical results.

For practical reason in the evaluation of the effective potential of the background field we parameterize the numerical results for  $\chi(p)$  by

$$\chi_{\text{para}}(p) = u(p)\chi_{\text{IR}}(p) + v(p)\chi_{\text{UV}}(p), \quad (154)$$

where  $\chi_{\text{IR}}(p)$  and  $\chi_{\text{UV}}(p)$  are defined by Eqs. (152) and (153), and  $u(p)$  and  $v(p)$  are smooth cut-off functions to restrict  $\chi_{\text{IR}}(p)$  and  $\chi_{\text{UV}}(p)$  to the IR and UV-regime, respectively. An optimal fit to the numerical results for  $\chi(p)$  is obtained with the choice

$$u(p) = \left[1 + \left(\frac{p}{\eta}\right)^m\right]^{-1}, \quad v(p) = 1 - \left(\frac{\lambda}{p^2 + \lambda}\right)^n. \quad (155)$$

From the best fit of Eq. (154) to the numerical data one extracts the following values for the parameters (for SU(2))

$$\begin{aligned} \eta &= 4.83M, & \lambda &= 89.62M^2 \\ m &= 3.13, & n &= 0.89. \end{aligned} \quad (156)$$

Fig. 1 shows also the fitted curve (154) together with the numerical data for  $\chi(p)$ . With  $\omega(p)$  and  $\chi(p)$  at hand we are now in a position to evaluate the effective potential of the Polyakov loop, see Eq. (162) below.

### VIII. THE EFFECTIVE POTENTIAL OF THE POLYAKOV LOOP

As discussed in Sect. II a constant background field  $a$  living in the Cartan algebra can serve as order parameter for confinement when it is directed along a compactified dimension. Thereby the inverse of the length  $L$  of the compactified dimension figures as temperature. In the Hamiltonian approach the effective potential of a spatial background field  $a$  is given by the energy density [29]

$$e(a, L) = \frac{\langle H \rangle_a}{V(d-1)}, \quad (157)$$

where  $\langle H \rangle_a$  is defined by the constrained variational problem (47) and given in the present approach by

Eq. (119). Furthermore,  $V$  is the spatial volume and for convenience we have divided the energy by the number of transversal spatial dimensions.

Assuming  $d = 3$  and compactifying the 3-axis to a circle with circumference  $L$  the above formulae all remain valid except for the following modifications: The integration over coordinate space reads

$$\int d^3x f(\mathbf{x}) = \int d^2x_{\perp} \int_0^L dx_3 f(\mathbf{x}_{\perp}, x_3), \quad (158)$$

where  $\mathbf{x}_{\perp}$  denotes the projection of  $\mathbf{x}$  onto the 1-2-plane. Accordingly the integration over momentum space becomes

$$\int d^3p f(\mathbf{p}) = \int d^2p_{\perp} \frac{1}{L} \sum_{n=-\infty}^{\infty} f(\mathbf{p}_{\perp}, p_n), \quad (159)$$

where

$$p_n = \frac{2\pi n}{L} \quad (160)$$

are the Matsubara frequencies and the shifted momentum variable  $\mathbf{p}_{\sigma}$  (142) reads

$$\mathbf{p}_{\sigma} = \mathbf{p}_{\perp} + (p_n - \sigma \mathbf{a}) \mathbf{e}_3, \quad (161)$$

With Eq. (159) we find from Eq. (119) for the energy density (157), using (122), (124) and (126)

$$\begin{aligned} e(a, L) &= \sum_{\sigma} \int d^3p (\omega^{\sigma}(\mathbf{p}) - \chi^{\sigma}(\mathbf{p})) \\ &= \sum_{\sigma} \int d^2p_{\perp} \frac{1}{L} \sum_n (\omega(p_{\sigma}) - \chi(p_{\sigma})), \end{aligned} \quad (162)$$

where  $p_{\sigma} = |\mathbf{p}_{\sigma}|$  is defined by Eq. (161). By shifting the summation index  $n$  one easily verifies that by Eq. (141) the potential (162) indeed has the periodicity property

$$e(\mathbf{a} + 4\pi/L\boldsymbol{\mu}, L) = e(\mathbf{a}, L) \quad (163)$$

required for the potential of the Polyakov loop by center symmetry.

For later use we calculate first the contributions to the effective potential arising from a gluon energy  $\omega(p_{\sigma})$  that obeys a power law

$$\omega_{\alpha}(p, \lambda) = M^{1-\alpha} \left(\sqrt{p^2 + \lambda}\right)^{\alpha}. \quad (164)$$

For later convenience we have introduced here an addition parameter  $\lambda \geq 0$ , which of course is irrelevant for  $p_{\sigma} \rightarrow \infty$ . Furthermore,  $M$  is a constant of dimension mass, which was introduced for dimensional reasons. For the  $\beta = 1$  solution of the variational calculation (see Sect. VII) the IR and UV behavior of  $\omega(k)$  is given by  $\omega_{\alpha=-1}(p, \lambda = 0)$  and  $\omega_{\alpha=1}(p, \lambda = 0)$ , respectively.

The contribution of  $\omega_{\alpha}(p_{\sigma}, \lambda)$  to the energy density (162)

$$e_{\alpha}(a, L, \lambda) := \sum_{\sigma} \int d^2p_{\perp} \frac{1}{L} \sum_n \omega_{\alpha}(p_{\sigma}, \lambda) \quad (165)$$

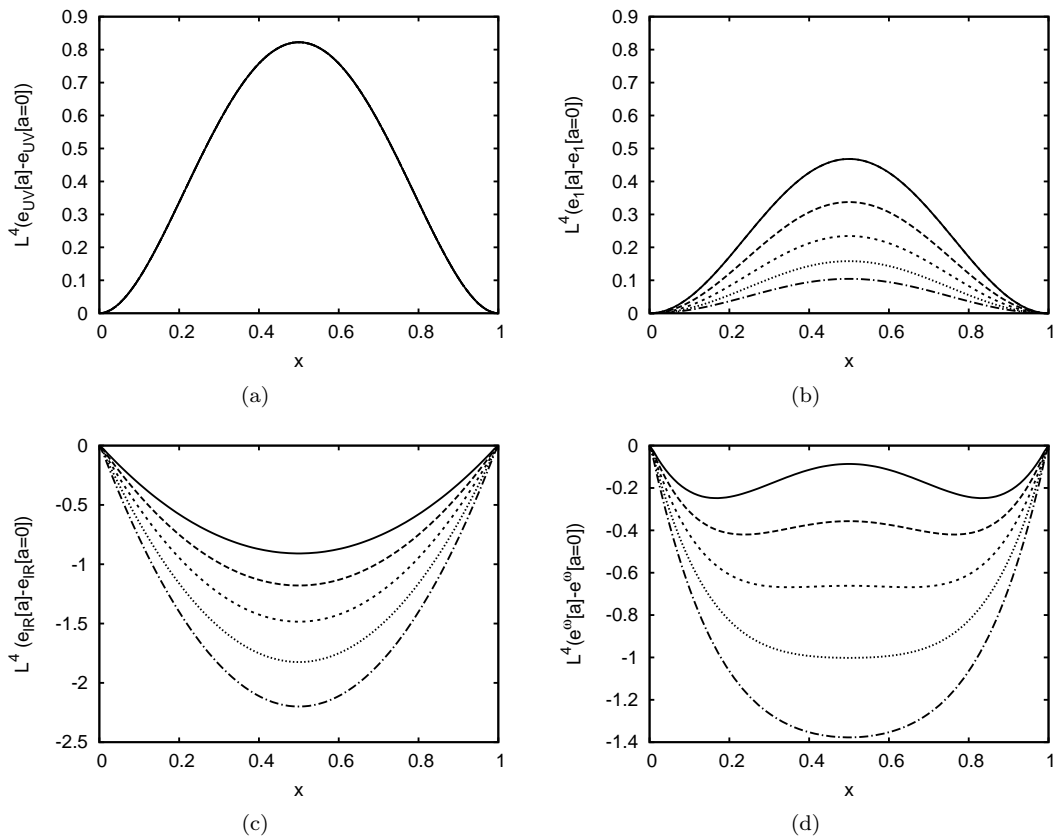


FIG. 2. The effective potential  $a(a, L)$  (162) multiplied by  $L^4$  at different temperatures  $L^{-1}$  for the gauge group  $SU(2)$ . The potential is shown as function of the dimensionless variable  $x$  (178), where  $\mathbf{a}\boldsymbol{\sigma} = a_3 = a$  for  $SU(2)$ , and for various forms of the gluon energy  $\omega(\mathbf{p})$  and neglecting the ghost loop,  $\chi(\mathbf{p}) = 0$ : (a) UV-(Weiss) potential (170)  $\omega(p) = p$ , (b) massive dispersion relation (173)  $\omega(p) = \sqrt{m^2 + p^2}$ , (c) IR-potential (176)  $\omega(p) = M^2/p$ , (d) the sum of the UV and IR potential,  $\omega(p) = p + M^2/p$ , which is obtained by adding the two potentials shown in (a) and (c).

is calculated in appendix B. One finds after the value of the potential at vanishing background field is subtracted, see Eq. (B12),

$$\begin{aligned} \bar{e}_\alpha(a, L, \lambda) &:= e_\alpha(a, L, \lambda) - e_\alpha(0, L, \lambda) \\ &= -\frac{8M^{1-\alpha}}{(4\pi)^{3/2}\Gamma(-\frac{\alpha}{2})} \\ &\times \sum_{\sigma} \sum_{n=1}^{\infty} \left(\frac{2\sqrt{\lambda}}{nL}\right)^{\frac{\alpha}{2}+\frac{3}{2}} \sin^2\left(\frac{n\sigma aL}{2}\right) K_{-\frac{\alpha}{2}-\frac{3}{2}}(nL\sqrt{\lambda}). \end{aligned} \quad (166)$$

where  $K_r(z)$  is the modified Bessel function (B11). For  $\lambda = 0$  the above expression simplifies to (see Eq. (B10))

$$\begin{aligned} \bar{e}_\alpha(a, L, \lambda = 0) &= -\frac{8M^{1-\alpha}}{(4\pi)^{3/2}} \frac{\Gamma(\frac{3}{2} + \frac{\alpha}{2})}{\Gamma(-\frac{\alpha}{2})} \\ &\times \left(\frac{2}{L}\right)^{3+\alpha} \sum_{\sigma>0} \sum_{n=1}^{\infty} \frac{1}{n^{3+\alpha}} \sin^2\left(\frac{n\sigma aL}{2}\right), \end{aligned} \quad (167)$$

where the summation is now over the positive roots only.

Before we give a full numerical calculation of the effective potential  $e(a, L)$  (162) let us discuss its qualitative features to reveal how the deconfinement phase transition shows up in this quantity. For this purpose we calculate below the IR and UV contributions to the effective potential. Note also that the momentum integrals (162) are UV divergent, so that the UV contributions require an analytic treatment to remove the divergences.

### A. Asymptotic contributions

For a first qualitative discussion of the Polyakov loop potential let us ignore the curvature  $\chi(p)$  in Eq. (162).  $\chi(p)$  is UV-subleading but has the same IR behavior as  $\omega(p)$ , see Sect. VII. Therefore, we expect a substantial change of the deconfinement phase transition temperature by ignoring  $\chi(p)$ . Nevertheless, in order to see how the deconfinement phase transition manifests itself in the effective potential it is enlightening to consider the simplified potential arising from (162) when the curvature  $\chi(p)$  is ignored. We first calculate the effective potential arising from the UV behavior of  $\omega(p)$ .

In the ultraviolet the gluon energy is given by  $\omega(p) = |\mathbf{p}|$ , which follows from Eq. (164) with  $\alpha = 1$  and  $\lambda = 0$ . For these values we obtain from Eqs. (165), (167)

$$\begin{aligned} \bar{e}_{\text{UV}}^\omega(a, L) &:= e_{\alpha=1}(a, L, \lambda = 0) - e_{\alpha=1}(0, L, \lambda = 0) \\ &= \frac{8}{\pi^2} \frac{1}{L^4} \sum_{\sigma > 0} \sum_{n=1}^{\infty} \frac{\sin^2(n\mathbf{a}\sigma L/2)}{n^4}. \end{aligned} \quad (168)$$

The summation over the Matsubara frequencies can be carried out for  $0 \leq \mathbf{a}\sigma L/2\pi \leq 1$  using

$$\sum_{n=1}^{\infty} \frac{\cos nx}{n^4} = \frac{\pi^4}{90} - \frac{\pi^2 x^2}{12} + \frac{\pi x^3}{12} - \frac{x^4}{48}, \quad 0 \leq x \leq 2\pi \quad (169)$$

which yields

$$\bar{e}_{\text{UV}}^\omega(a, L) = \frac{4}{3} \frac{\pi^2}{L^4} \sum_{\sigma > 0} \left( \frac{\mathbf{a}\sigma L}{2\pi} \right)^2 \left[ \frac{\mathbf{a}\sigma L}{2\pi} - 1 \right]^2. \quad (170)$$

This is precisely the Weiss potential, which is shown in Fig. 2(a) for the gauge group SU(2). It was originally obtained in Ref. [26] in a 1-loop calculation in Landau gauge. Thus, the present quasi-particle type approximation (165) to the gluons (cf. also Eq. (63)) with the gluon energy  $\omega(p)$  replaced by its ultraviolet limit, i.e. by the photon energy  $\omega_{\alpha=1}(p, \lambda = 0) = |\mathbf{p}|$ , is equivalent to an ordinary 1-loop background calculation. Since up to the periodicity (9) the Weiss potential is minimal only for  $a = 0$  we find for the Polyakov loop

$$\langle P[A_3] \rangle \simeq P[\langle A_3 \rangle = a = 0] = 1 \quad (171)$$

indicating the deconfined phase.

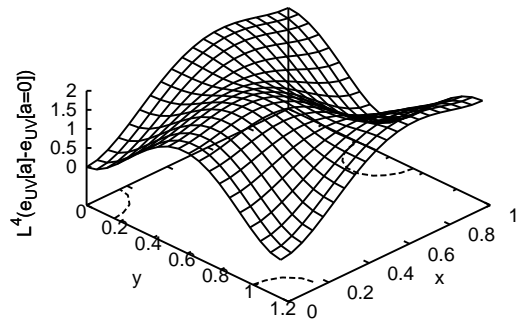
For the sake of illustration we also consider a massive gluon dispersion relation

$$\omega(p) = \sqrt{M^2 + p^2}, \quad (172)$$

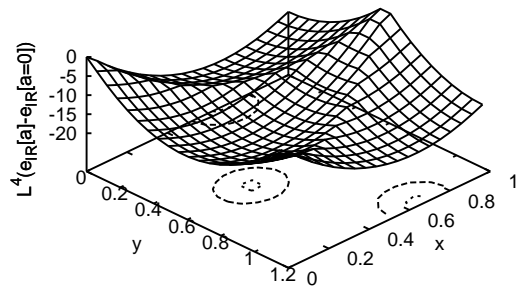
which is obtained in the variational approach to Yang-Mills theory in Coulomb gauge above the critical temperature of the deconfinement phase transition [17]. This dispersion relation follows from Eq. (164) for  $\alpha = 1$  and  $\lambda = M^2$ . With these parameter values we find from Eq. (166) for the effective potential

$$\begin{aligned} \bar{e}_1(a, L, M^2) &:= e_1(a, L, M^2) - e_1(0, L, M^2) \\ &= \frac{M^2}{2\pi^2} \sum_{\sigma} \sum_{n=1}^{\infty} \left( \frac{2}{nL} \right)^2 \sin^2(n\sigma\mathbf{a}L/2) K_{-2}(nLM). \end{aligned} \quad (173)$$

This potential is shown in Fig. 2(b) for SU(2). For  $M = 0$  this potential reduces, of course, to the Weiss potential shown in Fig. 2(a). Due to the presence of the energy scale  $M$  in Eq. (172) this potential is now temperature dependent. (The Weiss potential  $L^4 \bar{e}_{\text{UV}}^\omega$  is independent of  $L$ , see Fig. 2(a).) For any value of  $M$  this potential



(a)



(b)

FIG. 3. (a) The Weiss potential (170) and (b) the infrared potential (176) at  $L^{-1} = 290$  MeV for the gauge group SU(3) as a function of the dimensionless fields variables (178)  $x, y$  and multiplied by  $L^4$ . In both plots the local minima are marked by contours in the  $xy$ -plane.

is minimal at  $a = 0$  and gives rise to the same Polyakov loop as the Weiss potential.

The quasi-particle approximation to the energy density is, however, a priori non-perturbative. The gluon energy  $\omega(\mathbf{p})$  determined in the variational approach, in particular, captures the infrared confinement properties of the gluons. In the infrared the gluon energy (151) is given by Eq. (164) with  $\alpha = -1$  and  $\lambda = 0$ . For these values we find from Eq. (167)

$$\begin{aligned} \bar{e}_{\text{IR}}^\omega(a, L) &:= e_{\alpha=-1}(a, L, \lambda = 0) - e_{\alpha=-1}(0, L, \lambda = 0) \\ &= -4 \frac{M^2}{\pi^2} \frac{1}{L^2} \sum_{\sigma > 0} \sum_{n=1}^{\infty} \frac{1}{n^2} \sin^2(n\mathbf{a}\sigma L/2). \end{aligned} \quad (174)$$

The summation over  $n$  can be carried out for  $0 \leq \mathbf{a}\sigma L/2\pi < 1$  using

$$\sum_{n=1}^{\infty} \frac{\cos(nx)}{n^2} = \frac{\pi}{6} - \frac{\pi x}{2} + \frac{x^4}{4}, \quad 0 \leq x \leq 2\pi, \quad (175)$$

which yields

$$\bar{e}_{\text{IR}}^{\omega}(a, L) = 2 \frac{M^2}{L^2} \sum_{\sigma > 0} \left[ \left( \frac{\mathbf{a}\sigma L}{2\pi} \right)^2 - \frac{\mathbf{a}\sigma L}{2\pi} \right]. \quad (176)$$

This potential is shown in Fig. 2(c) for the gauge group SU(2). It drastically differs from the Weiss potential (168) obtained from the UV behavior of  $\omega(p)$  and shown in Fig. 2(a). First it has the opposite sign and second a non-trivial  $L$ -dependence. Its minimum occurs at  $a = \frac{\pi}{L}$  corresponding to a center symmetric ground state. Accordingly it yields a vanishing expectation value of the Polyakov loop (171).

$$\langle P[A_3] \rangle \simeq P \left[ \langle A_3 \rangle = a = \frac{\pi}{L} \right] = 0. \quad (177)$$

In Figs. 3 (a) and (b) the asymptotic UV and IR potentials (170) and (176), respectively, are shown for the gauge group SU(3) as function of the dimensionless variables

$$x := \frac{a_3 L}{2\pi}, \quad y := \frac{a_8 L}{2\pi}. \quad (178)$$

By the periodicity of the effective potential these variables can be restricted to the intervals

$$0 \leq x \leq 1, \quad 0 \leq y \leq \frac{2}{\sqrt{3}}. \quad (179)$$

As mentioned before, the Weiss potential  $L^4 \bar{e}_{\text{UV}}^{\omega}(a, L)$  is independent of the temperature  $L^{-1}$ , while the IR potential is temperature dependent and is shown in Fig. 3(b) for  $L^{-1} = 290$  MeV. The minima of the Weiss potential are degenerate and occur at field configurations  $a_{\text{min}}$ , for which the Polyakov line yields a center element  $z$

$$e^{-La_{\text{min}}} = z \in \mathbf{Z}(N), \quad (180)$$

and thus  $P[a_{\text{min}}] = z \neq 0$  as expected for the deconfined phase. For SU(3) the minima of the Weiss potential occur at (see Fig. 3(a))

$$(x_{\text{min}}, y_{\text{min}}) = (0, 0), \left(0, \frac{2}{\sqrt{3}}\right), \left(1, \frac{1}{\sqrt{3}}\right) \quad (181)$$

for which the Polyakov line is

$$e^{-La_{\text{min}}} = \mathbb{1}, \quad e^{i\frac{2\pi}{3}} \mathbb{1}, \quad e^{-i\frac{2\pi}{3}} \mathbb{1}. \quad (182)$$

The minima of the confining IR potential occur at center symmetric configurations, for which the Polyakov loop vanishes. For SU(2) this configuration is given by  $x_{\text{min}} = 1/2$  (see Fig. 2(c)) while for SU(3) these configurations read (see Fig. 3(b)):

$$(x_{\text{min}}, y_{\text{min}}) = \left(\frac{2}{3}, 0\right), \left(\frac{2}{3}, \frac{2}{\sqrt{3}}\right), \left(\frac{1}{3}, \frac{1}{\sqrt{3}}\right) \quad (183)$$

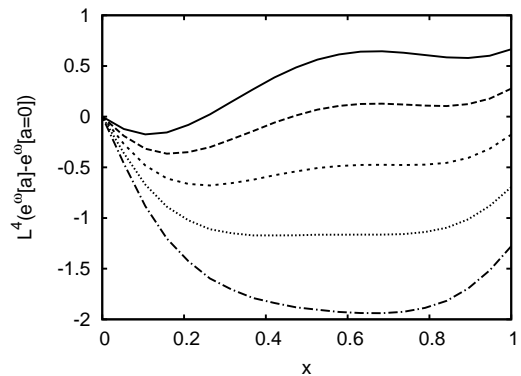


FIG. 4. The  $a_8 = 0$  slice of the potential (187) for the gauge group SU(3) as a function of  $x$  (178) for different  $L^{-1}$  in the range from 484 MeV to 880 MeV (from bottom to top). The critical temperature is 597 MeV.

and the corresponding Polyakov lines are given by

$$\begin{aligned} e^{-La_{\text{min}}} &= \text{diag} \left( e^{i\frac{2\pi}{3}}, e^{-i\frac{2\pi}{3}}, 1 \right), \\ &\text{diag} \left( e^{-i\frac{2\pi}{3}}, 1, e^{i\frac{2\pi}{3}} \right), \\ &\text{diag} \left( e^{i\frac{2\pi}{3}}, 1, e^{-i\frac{2\pi}{3}} \right) \end{aligned} \quad (184)$$

which all yield  $P[a_{\text{min}}] = 0$ .

## B. The deconfinement phase transition

Clearly the deconfinement phase transition is related to the transition in the effective potential from its IR behavior (174) to its UV behavior (168). To illustrate this let us approximate the Gribov formula (151) by

$$\sqrt{p^2 + \frac{M^4}{p^2}} \longrightarrow p + \frac{M^2}{p}, \quad (185)$$

i.e. we choose the gluon energy as

$$\omega(p) = \omega_{\alpha=1}(p, \lambda = 0) + \omega_{\alpha=-1}(p, \lambda = 0). \quad (186)$$

This expression is correct in both the IR and UV but certainly introduces an error in the mid-momentum regime, which influences the deconfinement phase transition. With Eq. (186) the energy density (162) for  $\chi(p) = 0$  becomes

$$\begin{aligned} \bar{e}^{\omega}(a, L) &= \bar{e}_{\text{IR}}^{\omega}(a, L) + \bar{e}_{\text{UV}}^{\omega}(a, L) \\ &= \frac{4}{\pi^2} \frac{1}{L^4} \sum_{n=1}^{\infty} \frac{1}{n^2} \left[ \frac{2}{n^2} - (ML)^2 \right] \sum_{\sigma > 0} \sin^2(n\mathbf{a}\sigma L/2) \end{aligned} \quad (187)$$

For SU(2) the only positive root is  $\sigma = 1$  and this potential can be expressed as

$$\bar{e}^{\omega}(a, L) = \frac{4}{3} \frac{\pi^2}{L^4} f(x), \quad f(x) = x^2(x-1)^2 + c(x^2 - x), \quad (188)$$

where

$$c := \frac{3M^2L^2}{2\pi^2} \quad (189)$$

and the variable  $x$  is defined in Eq. (178). For small temperatures  $L^{-1} \ll M$  this potential is negative and the system is in the confined phase. As  $L^{-1}$  increases the minimum of the potential at  $x = \frac{1}{2}$  turns into a maximum and the system makes a transition to the deconfined phase, see Fig. 2(d). In the relevant interval  $0 \leq x \leq 1$  the potential has a single minimum in the confined phase and two degenerate minima in the deconfined phase, which merge to the single minimum at  $x = \frac{1}{2}$  of the confined phase at the phase transition. Starting from the deconfined phase the phase transition occurs where the three roots of  $f'(x) = 0$  degenerate. This occurs for  $c = \frac{1}{2}$ , i.e. for

$$T_c = L^{-1} = \sqrt{3} \frac{M}{\pi}. \quad (190)$$

With the lattice result  $M = 880$  MeV this corresponds to  $T_c \approx 485$  MeV.

To exhibit the deconfinement phase transition for the gauge group SU(3) we cut the potential along a line which contains one of the degenerate minima both in the confined and deconfined phase. A convenient cut<sup>9</sup> is  $y = 0$ . Fig. 4 shows the  $y = 0$  (i.e.  $a_8 = 0$ ) cut through the potential (187). At low temperatures the minimum corresponds to the center symmetric configuration  $x = \frac{2}{3}$  ( $y = 0$ ). At a certain critical temperature this minimum disappears while a new minimum at a smaller  $x$ -value occurs, which (for sufficiently high temperature) eventually becomes the minimum  $x = y = 0$  for which the Polyakov loop equals the trivial center element  $z = \mathbb{1}$ . From Fig. 4 we find a critical temperature of  $T_c \approx 597$  MeV.

The critical temperatures obtained above are by far too high. Of course, given the approximations used to arrive at these values we do not expect a decent description of  $T_c$ . These approximations are: i) neglect of the curvature  $\chi(p)$  and ii) approximating Gribov's formula (185). The use of the correct Gribov formula (151) only slightly reduces  $T_c$  as long as the curvature is neglected as we will show now explicitly for the gauge group SU(2).

Using the Gribov formula (151) for  $\omega(k)$  but still neglect the curvature the effective potential (162) reads:

$$e_G^\omega(a, L) := \sum_\sigma \int d^2p_\perp \frac{1}{L} \sum_{n=-\infty}^{\infty} \omega_G(p_\sigma). \quad (191)$$

The evaluation of  $e_G^\omega(a, L)$  has to be done numerically. To avoid UV divergences we define

$$\bar{e}_G^\omega(a, L) := e_G^\omega(a, L) - e_G^\omega(a = 0, L) \quad (192)$$

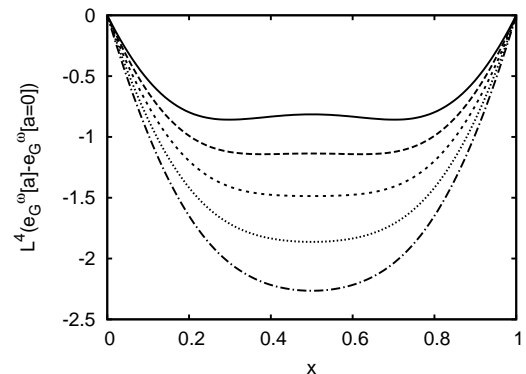


FIG. 5. The energy density (193) for the gauge group SU(2) as a function of the variable  $x$  (189) for different  $L^{-1}$  in the range from 360 to 480 MeV (from bottom to top). The phase transition occurs at a temperature of  $T_c \approx 432$  MeV.

and represent this quantity as

$$\begin{aligned} \bar{e}_G^\omega(a, L) &= [\bar{e}_G^\omega(a, L) - \bar{e}_{UV}^\omega(a, L)] + \bar{e}_{UV}^\omega(a, L) \\ &= \sum_\sigma \int d^3p \left\{ [\omega_G(\mathbf{p}_\sigma) - \omega_{\alpha=1}(\mathbf{p}_\sigma, \lambda = 0)] \right. \\ &\quad \left. - [\omega_G(\mathbf{p}_{\sigma=0}) - \omega_{\alpha=-1}(\mathbf{p}_{\sigma=0}, \lambda = 0)] \right\} + \bar{e}_{UV}^\omega(a, L) \end{aligned} \quad (193)$$

and calculate the integral numerically while using the analytic expression (170) in the last term. The resulting effective potential is shown in Fig. 5 for the gauge group SU(2) for several temperatures  $L^{-1}$ . One finds a critical temperature for the deconfinement phase transition of  $T_c \approx 432$  MeV, which is still much too high.

It is the omission of the curvature, which pushes the deconfinement phase transition to higher temperatures. This can be seen as follows: In the UV the curvature  $\chi(p)$  is suppressed by  $1/\ln p$  compared to the gluon energy  $\omega(p)$  and is in addition negative. Thus neglecting the curvature at most decreases the UV part of the potential, which is deconfining. In the deep IR the curvature  $\chi(p)$  agrees with  $\omega(p)$  (cf. Eqs. (151) and (152)). Neglecting here  $\chi(p)$  definitely increases the contribution of the confining IR potential. So in total, the neglect of the curvature  $\chi(p)$  decreases the deconfining part and at the same time increases the confining part of the potential. Both effects increase the transition temperature. This will be confirmed by the numerical results given in the next subsection. As we will explicitly see below the critical temperatures decreases substantially when the curvature  $\chi(p)$  is fully included.

### C. The full potential

Finally, we calculate the full effective potential (162) with the curvature  $\chi$  included. We first use the Gribov

<sup>9</sup> Alternative possible cuts are  $y = \frac{1}{\sqrt{3}}$  and  $y = \frac{2}{\sqrt{3}}$ .

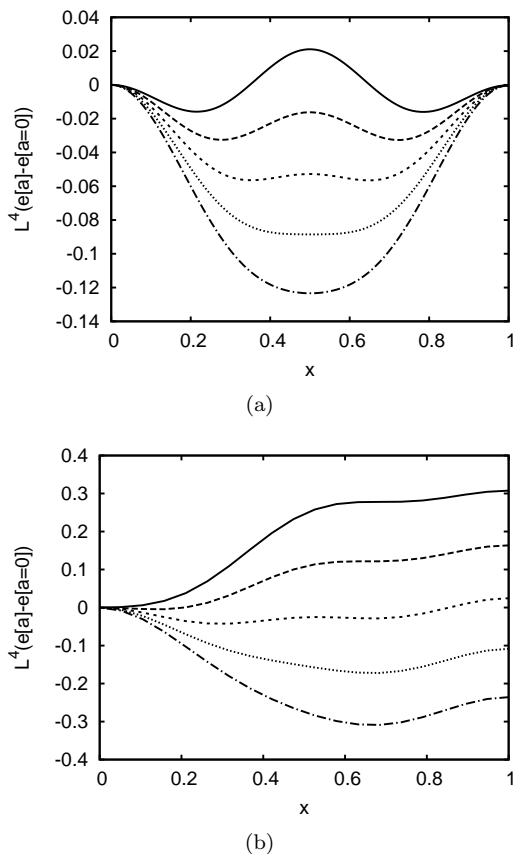


FIG. 6. The effective potential (194) for gauge group SU(2) (a) and the  $y = 0$  ( $a_8 = 0$ ) slice for SU(3) (b) as a function of  $x$  for different  $L^{-1}$  in the range from 260 to 290 MeV in figure (a) and from 260 MeV to 300 MeV in figure (b) (from bottom to top). We extract the following phase transition temperatures:  $T_c \approx 267$  MeV (SU(2)) and 278 MeV (SU(3)).

formula (151) for  $\omega(p)$  and in accord with the gap equation (145) for  $\chi(p)$  the IR expression  $\chi_{\text{IR}}(p)$  (152), which agrees with the IR behavior of  $\omega(p)$ . The energy density (162) then becomes

$$e(a, L) = \sum_{\sigma} \int d^3p [\omega_{\text{G}}(\mathbf{p}_{\sigma}) - \chi_{\text{IR}}(\mathbf{p}_{\sigma})]. \quad (194)$$

Subtracting the value at  $a = 0$  we have

$$\begin{aligned} \bar{e}(a, L) &= e(a, L) - e(a, L = 0) \\ &= \bar{e}_{\text{G}}^{\omega}(a, L) - \bar{e}_{\text{IR}}^{\omega}(a, L), \end{aligned} \quad (195)$$

where  $\bar{e}_{\text{G}}^{\omega}(a, L)$  and  $\bar{e}_{\text{IR}}^{\omega}(a, L)$  are defined in Eqs. (193) and (174), respectively. (The reader is advised to compare this expression to Eq. (187)!) The resulting potentials is shown in Fig. 6(a) for the gauge group SU(2), while Fig. 6(b) shows the  $a_8 = 0$  cut through the SU(3) potential for various temperatures  $L^{-1}$ . In both cases one observes a (deconfinement) phase transition, which, however, is first order for SU(2) and second order for SU(3). This is because at the deconfinement transition

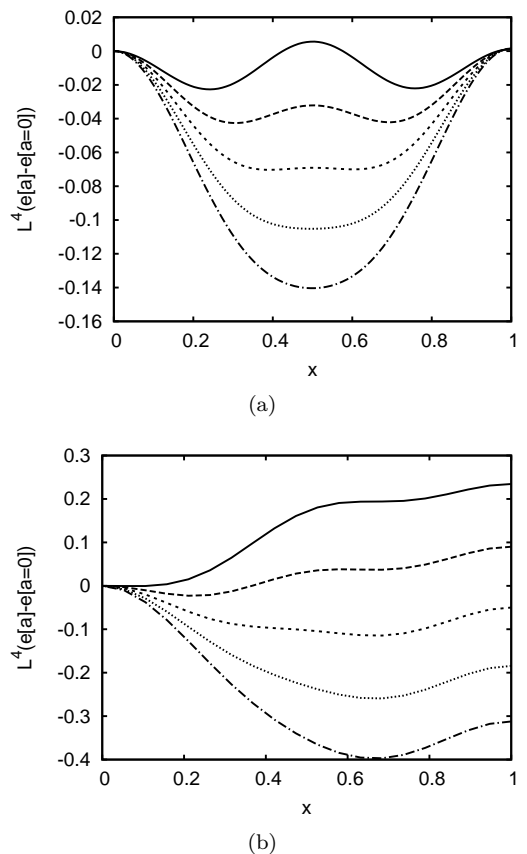


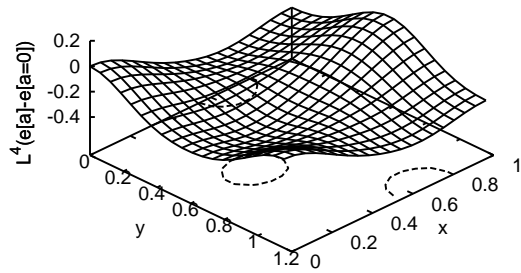
FIG. 7. The effective potential (196) for gauge group SU(2) (a) and the  $y = 0$  ( $a_8 = 0$ ) slice for SU(3) (b) as a function of  $x$  for different  $L^{-1}$  in the range from 260 to 290 MeV in figure (a) and from 260 MeV to 300 MeV in figure (b) (from bottom to top). We extract the following phase transition temperatures:  $T_c \approx 269$  MeV (SU(2)) and 283 MeV (SU(3)).

the position of the minimum of the potential changes continuously for SU(2) but discontinuously for SU(3). From these potentials one extracts a critical temperature of  $T_c \approx 267$  MeV and  $T_c \approx 277$  MeV for SU(2) and SU(3), respectively.

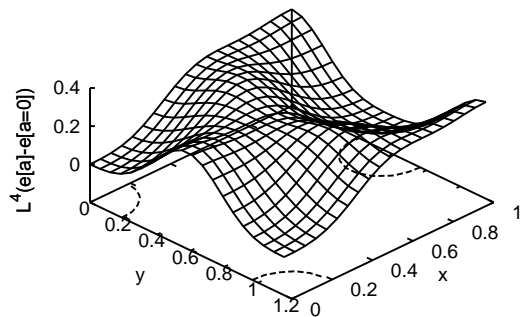
Alternatively we use for  $\chi(p)$  the parameterization (154) fitted to the numerical data and solve with this  $\chi(p)$  the gap equation (145) for  $\omega(p)$ . To avoid UV divergencies in the numerical calculations we represent the potential  $e(a, L)$  (162) in the form

$$\begin{aligned} e(a, L) &= \sum_{\sigma} \int d^3p [\omega(\mathbf{p}_{\sigma}) - \omega_{\alpha=1}(\mathbf{p}_{\sigma}, \lambda = 0) \\ &\quad - u(\mathbf{p}_{\sigma})\chi_{\text{IR}}(\mathbf{p}_{\sigma})] + e_{\alpha=1}(a, L, \lambda = 0)(a, L) \\ &\quad - \sum_{\sigma} \int d^3p v(\mathbf{p}_{\sigma})\chi_{\text{UV}}(\mathbf{p}_{\sigma}). \end{aligned} \quad (196)$$

The first integral can be straightforwardly carried out numerically. Using the explicit form of  $\chi_{\text{UV}}(p)$  (153) and  $v(p)$  (155) and the definition (164) we may write the last



(a)



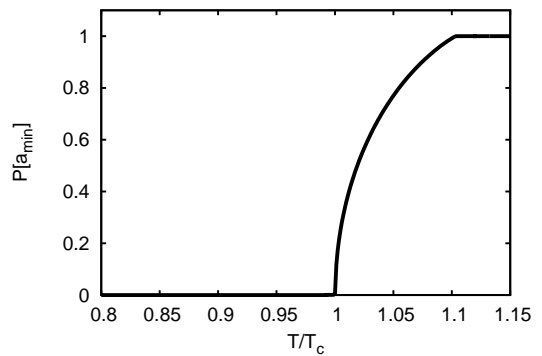
(b)

FIG. 8. The effective potential (194) for gauge group SU(3) as a function of  $x$  and  $y$  (a) below and (b) above the phase transition temperature. In both plots the local minima are marked by a contour in the  $xy$ -plane.

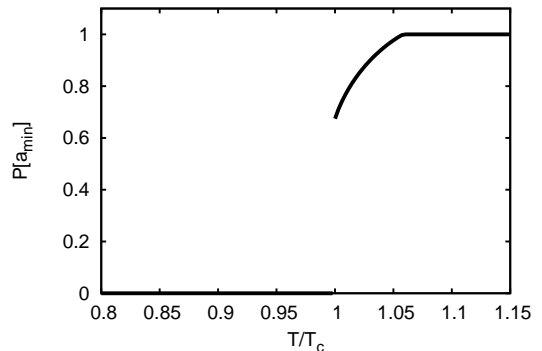
term as

$$\begin{aligned}
 & \sum_{\sigma} \int d^3 p v(\mathbf{p}_{\sigma}) \chi_{UV}(\mathbf{p}_{\sigma}) \\
 &= \sum_{\sigma} \left[ \int d^3 p \chi_{UV}(\mathbf{p}_{\sigma}) - \lambda^n \int d^3 p \frac{\chi_{UV}(\mathbf{p}_{\sigma})}{(\mathbf{p}_{\sigma}^2 + \lambda)^n} \right] \\
 &= e_{UV}^{\chi}(a, L) - \left( \frac{\lambda}{M^2} \right)^n \int_0^{\infty} dt e_{\alpha=1-2t-2n}(a, L, \lambda),
 \end{aligned} \tag{197}$$

where  $e_{UV}^{\chi}$  is defined by Eqs. (B14) of appendix B and  $e_{\alpha}(a, L, \lambda)$  is given by Eq. (166). The resulting effective potentials  $e(a, L)$  (196) are shown in Figs. 7(a) and 8 for the gauge group SU(2) and SU(3), respectively. Fig. 7(b) shows the  $y = 0$  cut through the SU(3) potential shown in Fig. 8 for various temperatures  $L^{-1}$ . Figs. 7(a) and 7(b) hardly differ from the potentials shown in Fig. 6(a) and 6(b), where the Gribov formula (151) was assumed for  $\omega(p)$  and the gap equation solved for  $\chi(p)$  yielding (152). The critical temperature found from Fig. 7 is  $T_c \approx 269$  MeV for SU(2) and  $T_c \approx 283$  MeV for SU(3). These critical temperatures only slightly differ



(a)



(b)

FIG. 9. The Polyakov loop  $\langle P[a] \rangle$  evaluated at the minimum  $a = a_{\min}$  of the full effective potential as a function of  $T/T_c$  for the gauge groups SU(2) (a) and SU(3) (b).

from the values found in Figs. 6 from Eq. (194). Within the given accuracy these values agree with the result of Ref. [17] where the variational approach to Yang–Mills theory in Coulomb gauge was directly extended to finite temperatures, studying the grand canonical ensemble. The present description has, however, the advantage that we do not need an additional variational ansatz for the density matrix of the gluons.

Finally, Fig. 9 (a) and (b) shows the Polyakov loop  $P[a_{\min}]$  as functions of the temperature obtained from the minima  $a_{\min}$  of the full effective potential for the gauge group SU(2) and SU(3), respectively. The order of the phase transition (second order for SU(2) and first order for SU(3)) is manifest in this figures.

## IX. CONCLUSIONS

In the present paper we have studied the deconfinement phase transition by investigating Yang–Mills theory for one compactified spatial dimension in the presence of an external background field directed along the compactified dimension and living in the Cartan subalgebra. In this formulation the inverse of the length  $L$  of

the compactified dimension represents the temperature. The vacuum energy density as a function of the constant background field serves as the effective potential of the Polyakov loop, the order parameter of confinement. We have calculated this potential within a variational approach by minimizing the energy density for given (value of the) background field and given compactified length  $L$ , using a Gaussian type ansatz for the vacuum wave functional and a background gauge fixing. This resulted in a set of coupled DSEs for the gluon and ghost propagators. We have shown that these equations can be reduced to the corresponding DSEs in Coulomb gauge at  $L^{-1} = 0$  and in the absence of the background field. However, the momenta along the compactified dimension have to be taken at the discrete Matsubara frequencies and are shifted by the background field. Using the zero-temperature results for the gluon and ghost propagators as input, from the effective potential of the Polyakov loop we have extracted a critical temperature for the deconfinement phase transition of  $T_c \approx 269$  MeV for SU(2) and  $T_c \approx 283$  MeV for SU(3). Within the given accuracy these values are consistent with the result of Ref. [17], where the variational approach to Yang–Mills theory in Coulomb gauge was extended to non-zero temperature by making a quasi-particle ansatz for the gluon density matrix and minimizing the free energy with respect to the quasi-gluon energy and the Fock basis. The presently calculated effective potential has also correctly revealed the order of the deconfinement phase transition for SU(2) and SU(3).

In the present approach the deconfinement phase transition is entirely determined by the zero-temperature propagators, which are defined as vacuum expectation values. This shows that the finite-temperature behavior of the theory, in particular the dynamics of the deconfinement phase transition, must be fully encoded in the vacuum wave functional, at least within the present truncation scheme.

The results obtained in the present paper are encouraging to extend the present approach to full QCD [15] at finite temperature and baryon density.

## ACKNOWLEDGMENTS

One of the authors (H.R.) acknowledges useful discussions with J.M. Pawłowski. We also thank D. Campagnari, M. Quandt and P. Watson for a critical reading of the manuscript and useful comments. This work was sup-

ported by DFG under contract DFG-Re 856/6-3, DFG-Re 856/9-1 and by BMBF under contract 06TU7199.

## Appendix A: Equations of motion

In this Appendix we show that the equations of motion resulting from the constrained variational approach (47), i.e. the gap equation and the ghost DSE, can be consistently solved for propagators of the form assumed in Eqs. (112), (113). As in the body of the paper we assume a constant background field living in the Cartan algebra. We first check that the form (112) is consistent with the symmetries of the gluon propagator. The symmetry relation (72) reads in momentum space

$$\mathcal{D}_{kl}^{ab}(\mathbf{p}) = \mathcal{D}_{lk}^{ba}(-\mathbf{p}). \quad (\text{A1})$$

Using

$$t_{kl}^{ab}(\mathbf{p}) = t_{lk}^{ba}(-\mathbf{p}), \quad (\text{A2})$$

Eq. (74) can be rewritten in momentum space as

$$t_{kk'}^{aa'}(\mathbf{p})\mathcal{D}_{k'l'}^{a'b'}(\mathbf{p})t_{l'l}^{b'b}(\mathbf{p}) = \mathcal{D}_{kl}^{ab}(\mathbf{p}). \quad (\text{A3})$$

Defining the gluon propagator in the spherical basis by Eqs. (103) and using (98), (100) the symmetry relation (A1) becomes in the spherical basis

$$\mathcal{D}_{kl}^{\mu\nu}(\mathbf{p}) = (-)^{\mu+\nu}\mathcal{D}_{lk}^{-\nu,-\mu}(-\mathbf{p}), \quad (\text{A4})$$

while using (105) Eq. (A3) reads

$$t_{kk'}^{\sigma}(\mathbf{p})\mathcal{D}_{k'l'}^{\sigma\tau}(\mathbf{p})t_{l'l}^{\tau}(\mathbf{p}) = \mathcal{D}_{kl}^{\sigma\tau}(\mathbf{p}). \quad (\text{A5})$$

Using Eq. (105) one easily convinces oneself that the diagonal ansatz (112) is compatible with Eqs. (A4) and (A5).

Next we analyse the equations of motion, i.e. the ghost DSE (77) and the gap equation (93) together with the expressions (79) for the ghost self-energy and (87) for the curvature. We start with the ghost DSE (77).

### 1. The ghost self-energy

Rewriting the ghost self-energy (84) in momentum space

$$\Sigma(\mathbf{p}) = \int \hat{d}q t_{kk'}^{aa'}(-\mathbf{q})t_{l'l}^{bb'}(\mathbf{q})\mathcal{D}_{l'k'}^{b'a'}(\mathbf{q})\hat{T}_a\hat{d}_{k'}(\mathbf{p}+\mathbf{q})\hat{G}(\mathbf{p}+\mathbf{q})\hat{T}_b\hat{d}_l(\mathbf{p}). \quad (\text{A6})$$

and switching to the spherical basis defined by Eqs. (103) we find

$$\Sigma^{\sigma\tau}(\mathbf{p}) = (-)^{\sigma'+\tau'}\hat{T}_{-\sigma'\mu\sigma}^*\hat{T}_{-\tau'\nu\tau} \int \hat{d}qt_{l'l}^{\nu}(\mathbf{q})\mathcal{D}_{l'k'}^{\nu\mu}(\mathbf{q})t_{k'k}^{\mu}(\mathbf{q})d_k^{\sigma}(\mathbf{p}+\mathbf{q})G^{\sigma'\tau'}(\mathbf{p}+\mathbf{q})d_l^{\tau}(\mathbf{p}), \quad (\text{A7})$$

where we have also defined the structure constant  $\hat{T}_b^{ac} = \epsilon^{abc}$  in the spherical basis

$$\begin{aligned} \hat{T}_{\rho\sigma\tau} &= \epsilon^{abc}\langle a|\rho\rangle\langle b|\sigma\rangle\langle c|\tau\rangle \\ &= \epsilon^{abc}e_{\rho}^ae_{\sigma}^be_{\tau}^c = \mathbf{e}_{\rho}(\mathbf{e}_{\sigma} \times \mathbf{e}_{\tau}). \end{aligned} \quad (\text{A8})$$

Using Eq. (101) we obtain

$$\hat{T}_{\rho\sigma\tau} = -i\epsilon_{\rho\sigma\tau}. \quad (\text{A9})$$

Here the totally anti-symmetric tensor  $\epsilon_{\rho\sigma\tau}$  is defined as usual, however, for the indices  $\sigma = -1, 0, 1$ . Since the indices  $\rho, \sigma, \tau, \dots$  take the values  $0, \pm 1$  the totally anti-symmetric tensor  $\epsilon_{\rho\sigma\tau}$  is non-zero only for

$$\rho + \sigma + \tau = 0. \quad (\text{A10})$$

Assuming in Eq. (A7) color diagonal propagators (112), (113) we obtain

$$\begin{aligned} \Sigma^{\sigma\tau}(\mathbf{p}) &= -\hat{T}_{-\sigma'\mu\sigma}\hat{T}_{-\sigma'\mu\tau} \\ &\times \int \bar{d}q t_{lk}^\mu(\mathbf{q})\mathcal{D}^\mu(\mathbf{q})d_k^\sigma(\mathbf{p}+\mathbf{q})G^{\sigma'}(\mathbf{p}+\mathbf{q})d_l^{\tau'}(\mathbf{p}), \end{aligned} \quad (\text{A11})$$

where we have used

$$t_{l'l'}^\mu(\mathbf{q})t_{l'k'}^\mu(\mathbf{q})t_{k'l}^\mu(\mathbf{q}) = t_{lk}^\mu(\mathbf{q}). \quad (\text{A12})$$

Since (no summation over  $\rho, \mu$ ),

$$\hat{T}_{-\rho\mu\sigma}^*\hat{T}_{-\rho\mu\tau} = \delta_{\sigma\tau} |T_{-\rho\mu\sigma}|^2. \quad (\text{A13})$$

the ghost self-energy becomes indeed color diagonal

$$\Sigma^{\sigma\tau}(\mathbf{p}) = \delta^{\sigma\tau}\Sigma^\sigma(\mathbf{p}), \quad (\text{A14})$$

where

$$\begin{aligned} \Sigma^\sigma(\mathbf{p}) &= -\left|\hat{T}_{-\tau\mu\sigma}\right|^2 \\ &\times \int \bar{d}q d_l^\sigma(\mathbf{p})t_{lk}^\mu(\mathbf{q})d_k^{\tau'}(\mathbf{p}+\mathbf{q})\mathcal{D}^\mu(\mathbf{q})G^\tau(\mathbf{p}+\mathbf{q}). \end{aligned} \quad (\text{A15})$$

With the explicit form of  $d^\sigma(\mathbf{p})$  (107) we have

$$d_k^{\tau'}(\mathbf{p}+\mathbf{q}) = d_k^\mu(\mathbf{q}) + d_k^{\tau-\mu}(\mathbf{p}). \quad (\text{A16})$$

Using furthermore that

$$d_k^\mu(\mathbf{q})t_{kl}^\mu(\mathbf{q}) = 0 \quad (\text{A17})$$

we can rewrite the ghost self-energy (A15) as

$$\begin{aligned} \Sigma^\sigma(\mathbf{p}) &= -|T_{-\tau\mu\sigma}|^2 \\ &\times \int \bar{d}q d_l^\sigma(\mathbf{p})t_{lk}^\mu(\mathbf{q})d_k^{\tau-\mu}(\mathbf{p})\mathcal{D}^\mu(\mathbf{q})G^\tau(\mathbf{q}+\mathbf{p}). \end{aligned} \quad (\text{A18})$$

The antisymmetric tensor  $\hat{T}_{-\tau\mu\sigma}$  is non-vanishing only for  $\mu + \sigma - \tau = 0$ . Due to this sum rule the summation over  $\tau$  can be explicitly carried out yielding with

$$\left|\hat{T}_{-(\mu+\sigma)\mu\sigma}\right|^2 = 1 \quad (\text{A19})$$

the final expression

$$\begin{aligned} \Sigma^\sigma(\mathbf{p}) &= \\ &= -\sum_\mu \int \bar{d}q d_l^\sigma(\mathbf{p})t_{lk}^\mu(\mathbf{q})d_l^\sigma(\mathbf{p})\mathcal{D}^\mu(\mathbf{q})G^{\sigma+\mu}(\mathbf{p}+\mathbf{q}). \end{aligned} \quad (\text{A20})$$

Note this quantity is positive definite since the  $d_k^\sigma(\mathbf{p})$  (107) are purely imaginary. With Eq. (A14) the ghost DSE (77) becomes in the spherical basis

$$G^{\sigma^{-1}}(\mathbf{p}) = G_0^{\sigma^{-1}}(\mathbf{p}) - \Sigma^\sigma(\mathbf{p}), \quad (\text{A21})$$

where

$$G_0^{\sigma^{-1}}(\mathbf{p}) = -\mathbf{d}^\sigma(\mathbf{p})\mathbf{d}^\sigma(\mathbf{p}) = (\mathbf{p} - \mathbf{e}_3\sigma a)^2 \quad (\text{A22})$$

and  $\Sigma^\sigma(\mathbf{p})$  is defined by Eq. (A20). This shows that the diagonal ansatz, Eqs. (112), (113) for the propagators is indeed compatible with the ghost DSE. What remains to be done is to show that this ansatz is also compatible with the gap equation (93). For this purpose we investigate first the curvature  $\chi(\mathbf{q})$ , which enters the gap equation.

## 2. The curvature

Fourier transforming the curvature (87) we find

$$\begin{aligned} \chi_{kl}^{ab}(\mathbf{p}) &= \frac{1}{2}t_{kk'}^{aa'}(\mathbf{p})t_{l'l'}^{bb'}(-\mathbf{p}) \\ &\times \int \bar{d}q \text{tr} \left( \hat{T}_{a'}\hat{d}_{k'}(\mathbf{p}+\mathbf{q})G(\mathbf{p}+\mathbf{q})\hat{T}_{b'}\hat{d}_{l'}(\mathbf{q})G(\mathbf{q}) \right). \end{aligned} \quad (\text{A23})$$

Rewriting this expression in the spherical basis (103) and assuming a color diagonal ghost propagator (113) we obtain

$$\begin{aligned} \chi_{kl}^{\mu\nu}(\mathbf{p}) &= -\hat{T}_{-\tau\mu\sigma}^*\hat{T}_{-\tau\nu\sigma} \\ &\times \int \bar{d}q t_{kk'}^\mu(\mathbf{p})d_{k'}^{\tau'}(\mathbf{q}+\mathbf{p})d_{l'}^\sigma(\mathbf{q})t_{l'l}^\nu(\mathbf{p})G^\sigma(\mathbf{q})G^\tau(\mathbf{q}+\mathbf{p}). \end{aligned} \quad (\text{A24})$$

With (A13) we find that the curvature is also color diagonal in the spherical basis

$$\chi_{kl}^{\mu\nu}(\mathbf{p}) = \delta^{\mu\nu}\chi_{kl}^\mu(\mathbf{p}). \quad (\text{A25})$$

Using (A16) and the sum rule for the indices of  $\hat{T}_{-\tau\mu\sigma}$  the summation over  $\tau$  can be trivially carried out, yielding

$$\begin{aligned} \chi_{kl}^\mu(\mathbf{p}) &= \\ &= -\int \bar{d}p t_{kk'}^\mu(\mathbf{p})d_{k'}^\sigma(\mathbf{q})d_{l'}^\sigma(\mathbf{q})t_{l'l}^\mu(\mathbf{p})G^\sigma(\mathbf{q})G^{\mu+\sigma}(\mathbf{q}+\mathbf{p}). \end{aligned} \quad (\text{A26})$$

Consider now the Lorentz structure of  $\chi_{kl}^\mu(\mathbf{p})$ . By its definition as derivative with respect to the (transversal) gauge field this quantity has to be transverse as well. Indeed from the explicit expression (A26) it is seen that it satisfies the transversality condition

$$t_{mk}^\mu(\mathbf{p})\chi_{kl}^\mu(\mathbf{p})t_{ln}^\mu(\mathbf{p}) = \chi_{mn}^\mu(\mathbf{p}). \quad (\text{A27})$$

From this we can conclude that it has the form<sup>10</sup>

$$\chi_{kl}^\mu(\mathbf{p}) = \frac{1}{g^2} t_{kl}^\mu(\mathbf{p}) \chi^\mu(\mathbf{p}), \quad (\text{A28})$$

where the scalar curvature  $\chi^\mu(\mathbf{p})$  can be obtained as

$$\chi^\mu(\mathbf{p}) = \frac{g^2}{d-1} t_{lk}^\mu(\mathbf{p}) \chi_{kl}^\mu(\mathbf{p}). \quad (\text{A29})$$

Here  $d$  is the number of spatial dimensions and we have used

$$\hat{t}_{kk}^\mu(\mathbf{p}) = d - 1. \quad (\text{A30})$$

Inserting here the explicit expression (A26) and using  $t_{ll'}^\mu(\mathbf{p}) = t_{l'l}^\mu(\mathbf{p})$  we obtain

$$\begin{aligned} \chi^\mu(\mathbf{p}) &= -\frac{g^2}{2(d-1)} \\ &\times \sum_{\sigma} \int \bar{d}q d_k^\sigma(\mathbf{q}) t_{kl}^\mu(\mathbf{p}) d_l^\sigma(\mathbf{q}) G^\sigma(\mathbf{q}) G^{\mu+\sigma}(\mathbf{p} + \mathbf{q}). \end{aligned} \quad (\text{A31})$$

Eqs. (A25) and (A28) show that in the spherical basis the curvature  $\chi(q)$  is not only color diagonal but has also the same Lorentz structure as assumed for the gluon propagator (112).

### 3. The gap equation

Consider now the gap equation (93), which after Fourier transformation becomes

$$\begin{aligned} \frac{g^2}{4} \mathcal{D}^{-1}(\mathbf{p}) \mathcal{D}^{-1}(\mathbf{p}) \\ = \frac{1}{g^2} \left( -\hat{t}(\mathbf{p}) \hat{\mathbf{d}}(\mathbf{p}) \hat{\mathbf{d}}(\mathbf{p}) \hat{t}(\mathbf{p}) \right) + g^2 \chi(\mathbf{p}) \chi(\mathbf{p}). \end{aligned} \quad (\text{A32})$$

This is still a matrix equation both in the adjoint color and Lorentz indices. Rewriting this equation in the spherical basis defined by Eq.(103) and using Eqs. (104) and (A25) we observe that the gluon propagator  $\mathcal{D}(\mathbf{p})$  has indeed to be color diagonal and obtain

$$\begin{aligned} \frac{g^4}{4} \mathcal{D}^\sigma(\mathbf{p})^{-1} \mathcal{D}^\sigma(\mathbf{p})^{-1} \\ = (-t^\sigma(\mathbf{p}) \mathbf{d}^\sigma(\mathbf{p}) \mathbf{d}^\sigma(\mathbf{p}) t^\sigma(\mathbf{p})) + g^4 \chi^\sigma(\mathbf{p}) \chi^\sigma(\mathbf{p}). \end{aligned} \quad (\text{A33})$$

Here  $\mathcal{D}^\sigma(\mathbf{p})^{-1}$  and  $\chi^\sigma(\mathbf{p})$ , like  $t^\sigma(\mathbf{p})$ , are still Lorentz matrices. This equation is compatible with the Lorentz

structure of the gluon propagator assumed in (112), which resulted in the Lorentz structure (A28) of the curvature. Thus the ansätze (112), (113) for the propagators are also compatible with the gap equation. We have thus shown that the equation of motions resulting from the constraint variational principle  $\langle H \rangle_a \rightarrow \min$ ,  $\langle A \rangle_a = a$  in the background gauge (67) allow for color diagonal solutions. For such solutions we find for the energy density (94) at the stationary point

$$\begin{aligned} \langle H_K + H_B^A \rangle_a \\ = g^2 V \sum_{\sigma} \int \bar{d}q \left( \frac{1}{2} \mathcal{D}^\sigma(\mathbf{q})^{-1} - \chi^\sigma(\mathbf{q}) \right), \end{aligned} \quad (\text{A34})$$

where  $V$  is the spatial volume and  $\mathcal{D}^\sigma(p)$  and  $\chi^\sigma(p)$  are still Lorentz matrices. Carrying out the trace over the Lorentz indices thereby using Eqs. (112) and (A28) we obtain

$$\begin{aligned} \langle H_K + H_B^A \rangle_a \\ = (d-1)V \sum_{\sigma} \int \bar{d}q \left( \frac{g^2}{2} \mathcal{D}^\sigma(\mathbf{q})^{-1} - \chi^\sigma(\mathbf{q}) \right), \end{aligned} \quad (\text{A35})$$

where  $\mathcal{D}^\sigma(\mathbf{p})$  and  $\chi^\sigma(\mathbf{p})$  are now Lorentz scalars. (Note by Eq. (A28) the Lorentz tensor  $\chi_{kl}^\sigma(\mathbf{p})$  and the Lorentz scalar  $\chi^\sigma(\mathbf{p})$  differ by a factor of  $g^2$ .)

### Appendix B: The energy density

Below we calculate the contribution of the generic gluon energy (164) to the energy density (165). Representing

$$\left( \sqrt{p_\sigma^2 + \lambda} \right)^\alpha = \left( \mathbf{p}_\perp^2 + (p_n - \sigma \mathbf{a})^2 + \lambda \right)^{\alpha/2} \quad (\text{B1})$$

by a proper-time integral<sup>11</sup>

$$(p_\sigma^2 + \lambda)^{\alpha/2} = \frac{1}{\Gamma(-\frac{\alpha}{2})} \int_0^\infty d\tau \tau^{-1-\frac{\alpha}{2}} e^{-\tau(p_\sigma^2 + \lambda)} \quad (\text{B2})$$

we find for the energy density (165)

$$\begin{aligned} e_\alpha(a, L, \lambda) &= \frac{M^{1-\alpha}}{4\pi} \frac{1}{\Gamma(-\frac{\alpha}{2})} \\ &\times \sum_{\sigma} \frac{1}{L} \sum_n \int_0^\infty dx \int_0^\infty d\tau \tau^{-1-\frac{\alpha}{2}} e^{-\tau[x + (k_n - \sigma \mathbf{a})^2]} e^{-\lambda \tau}. \end{aligned} \quad (\text{B3})$$

Here we have carried out the integral over the azimuthal angle of  $\mathbf{p}_\perp$  and set  $x = \mathbf{p}_\perp^2$ . The integral over  $x$  can

<sup>10</sup> The transversal projector  $t_{kl}^\mu(\mathbf{p})$  will explicitly show up after the angular integral in (A26) is carried out. Furthermore, the factor  $g^2$  has been explicitly included so that  $\chi^\mu(q)$  reduces for  $\mu = 0$  to the curvature defined in Ref. [6], see Sect. VI C.

<sup>11</sup> We assume here that  $\alpha$  is such that the proper-time integral exists, otherwise  $\int_0^\infty d\tau$  has to be replaced by  $\int_{1/\Lambda^2}^\infty d\tau$ , where  $\Lambda$  is a UV cut-off.

be carried out yielding a factor  $\tau^{-1}$ . By means of the Poisson resummation formula one derives the relation

$$\frac{1}{L} \sum_n f(p_n) = \frac{1}{2\pi} \int_{-\infty}^{\infty} dz f(z) \sum_n e^{inzL}, \quad p_n = \frac{2n\pi}{L}. \quad (\text{B4})$$

Using this relation in Eq. (B3) and performing the integration over  $z$  we obtain

$$e_\alpha(a, L, \lambda) = \frac{M^{1-\alpha}}{(4\pi)^{3/2}} \frac{1}{\Gamma(-\frac{\alpha}{2})} \times \sum_\sigma \sum_{n=-\infty}^{\infty} e^{in\sigma a L} \int_0^\infty d\tau \tau^{-\frac{5}{2}-\frac{\alpha}{2}} e^{-\frac{1}{\tau}(\frac{nL}{2})^2} e^{-\lambda\tau}. \quad (\text{B5})$$

Obviously the proper-time integral is not well-defined for  $\lambda = 0$  and  $n = 0$ . Fortunately, this term drops out by subtracting the energy density at vanishing background

$$\bar{e}_\alpha(a, L, \lambda) = -4(4\pi)^{-3/2} \frac{M^{1-\alpha}}{\Gamma(-\frac{\alpha}{2})} \sum_\sigma \sum_{n=1}^{\infty} \left(\frac{2}{nL}\right)^{\alpha+3} \sin^2\left(n\frac{\sigma a L}{2}\right) \int_0^\infty ds s^{\frac{1}{2}+\frac{\alpha}{2}} e^{-s} e^{-\frac{\lambda}{s}(\frac{nL}{2})^2}. \quad (\text{B8})$$

For  $\lambda = 0$  the remaining integral can be expressed by Euler's Gamma-function

$$\bar{e}_\alpha(a, L, \lambda = 0) = -\frac{4M^{1-\alpha}}{(4\pi)^{3/2}} \frac{\Gamma(\frac{3}{2} + \frac{\alpha}{2})}{\Gamma(-\frac{\alpha}{2})} \times \sum_\sigma \left(\frac{2}{L}\right)^{3+\alpha} \sum_{n=1}^{\infty} \frac{1}{n^{3+\alpha}} \sin^2(n\sigma a L/2). \quad (\text{B9})$$

Obviously, the vanishing roots  $\sigma = (0, 0)$  do not contribute to the potential difference  $e_\alpha(a) - e_\alpha(a = 0)$ . Furthermore, the negative roots give the same contribution as the positive ones. We can therefore restrict the summation over  $\sigma$  to the positive roots  $\sigma > 0$  and take care of the contribution of the negative roots by an additional factor 2. This yields

$$\bar{e}_\alpha(a, L, \lambda = 0) = -8 \frac{M^{1-\alpha}}{(4\pi)^{3/2}} \frac{\Gamma(\frac{3}{2} + \frac{\alpha}{2})}{\Gamma(-\frac{\alpha}{2})} \left(\frac{2}{L}\right)^{3+\alpha} \times \sum_{\sigma>0} \sum_{n=1}^{\infty} \frac{1}{n^{3+\alpha}} \sin^2(n\sigma a L/2). \quad (\text{B10})$$

For  $\lambda \neq 0$  the remaining proper-time integral in Eq. (B8) cannot be taken analytically but can be expressed by a

field

$$\begin{aligned} \bar{e}_\alpha(a, L, \lambda) &:= e_\alpha(a, L, \lambda) - e_\alpha(a = 0, L, \lambda) \\ &= \frac{M^{1-\alpha}}{(4\pi)^{3/2}} \frac{2}{\Gamma(-\frac{\alpha}{2})} \\ &\times \sum_\sigma \sum_{n=1}^{\infty} [\cos(n\sigma a L) - 1] \int_0^\infty d\tau \tau^{-\frac{5}{2}-\frac{\alpha}{2}} e^{-\frac{1}{\tau}(\frac{nL}{2})^2} e^{-\lambda\tau}. \end{aligned} \quad (\text{B6})$$

With a change of variable  $s = (nL/2)^2/\tau$  in the proper-time integral

$$\begin{aligned} \int_0^\infty d\tau \tau^{-\frac{5}{2}-\frac{\alpha}{2}} e^{-\frac{1}{\tau}(\frac{nL}{2})^2} e^{-\lambda\tau} \\ = \left(\frac{2}{nL}\right)^{3+\alpha} \int_0^\infty ds s^{\frac{1}{2}+\frac{\alpha}{2}} e^{-s} e^{-\frac{\lambda}{s}(\frac{nL}{2})^2} \end{aligned} \quad (\text{B7})$$

we find for the energy density (B6) after some trivial algebraic manipulations

modified Bessel function  $K_\nu(z)$

$$\begin{aligned} \int_0^\infty ds s^{-1-t} e^{-s} \exp\left[-\frac{\lambda}{s} \left(\frac{nL}{2}\right)^2\right] \\ = 2 \left(\frac{2}{Ln\sqrt{\lambda}}\right)^t K_t(nL\sqrt{\lambda}), \end{aligned} \quad (\text{B11})$$

yielding

$$\begin{aligned} \bar{e}_\alpha(a, L, \lambda) &= -8 \frac{M^{1-\alpha}}{(4\pi)^{3/2} \Gamma(-\frac{\alpha}{2})} \\ &\times \sum_\sigma \sum_{n=1}^{\infty} \left(\frac{2\sqrt{\lambda}}{nL}\right)^{\frac{\alpha}{2}+\frac{3}{2}} \sin^2(\sigma a L/2) K_{-\frac{\alpha}{2}-\frac{3}{2}}(nL\sqrt{\lambda}). \end{aligned} \quad (\text{B12})$$

As in the previous case  $\lambda = 0$ , the summation over  $\sigma$  can be restricted to  $\sigma > 0$  by including a factor of 2.

To eliminate the UV divergencies from the energy density  $e(a, L)$  (162) we also need to isolate the contribution from the UV behavior of  $\chi$ . The UV form of  $\chi$  is given by Eq. (153). Using

$$\frac{1}{\ln \frac{p_\sigma^2 + \lambda}{M^2}} = \int_0^\infty dt \left(\frac{M^2}{p_\sigma^2 + \lambda}\right)^t, \quad p_\sigma^2 + \lambda > M^2 \quad (\text{B13})$$

and the definition (164) of  $\omega_\alpha(p, M, \lambda)$  we have

$$\chi_{\text{UV}}(p) = \int_0^\infty dt \omega_{\alpha=1-2t}(p, \lambda). \quad (\text{B14})$$

With this relation the (negative of the) energy contribution generated by the UV-behavior of  $\chi$  reads

$$e_{\text{UV}}^{\chi}(a, L) := \sum_{\sigma} \int \mathrm{d}p \chi_{\text{UV}}(p_{\sigma}) \quad (\text{B15})$$

$$= \int_0^{\infty} dt e_{\alpha=1-2t}(a, L, \lambda),$$

---

where  $e_{\alpha}(a, L, \lambda)$  is defined in Eq. (B3). Subtracting the  $a = 0$  contribution and using Eq. (166) we obtain

$$e_{\text{UV}}^{\chi}(a, L) - e_{\text{UV}}^{\chi}(a = 0, L) = -\frac{8}{(4\pi)^{3/2}} \int_0^{\infty} dt \frac{M^{2t}}{\Gamma(t - \frac{1}{2})} \left(\frac{\sqrt{\lambda}}{L}\right)^{2-t} \sum_{\sigma} \sum_{n=1}^{\infty} \left(\frac{2}{n}\right)^{2-t} \sin^2\left(n\sigma\mathbf{a}\frac{L}{2}\right) K_{t-2}(nL\sqrt{\lambda}) \quad (\text{B16})$$

and after restricting the summation over  $\sigma$  to positive roots

$$e_{\text{UV}}^{\chi}(a, L) - e_{\text{UV}}^{\chi}(a = 0, L) = -\frac{16}{(4\pi)^{3/2}} \int_0^{\infty} dt \frac{M^{2t}}{\Gamma(t - \frac{1}{2})} \left(\frac{\sqrt{\lambda}}{L}\right)^{2-t} \sum_{\sigma>0} \sum_{n=1}^{\infty} \left(\frac{2}{n}\right)^{2-t} \sin^2\left(n\sigma\mathbf{a}\frac{L}{2}\right) K_{t-2}(nL\sqrt{\lambda}). \quad (\text{B17})$$


---

- |   |  |
|---|--|
| <p>[1] B. Svetitsky and L. G. Yaffe, Nucl. Phys. <b>B210</b>, 423 (1982).</p> <p>[2] F. Karsch, Lect. Notes Phys. <b>583</b>, 209 (2002).</p> <p>[3] C. S. Fischer, J.Phys.G <b>G32</b>, R253 (2006).</p> <p>[4] J. M. Pawłowski, Annals Phys. <b>322</b>, 2831 (2007).</p> <p>[5] P. Watson and H. Reinhardt, Phys. Rev. <b>D75</b>, 045021 (2007), Phys. Rev. <b>D85</b>, 025014 (2012).</p> <p>[6] C. Feuchter and H. Reinhardt, Phys. Rev. <b>D70</b>, 105021 (2004); arXiv:hep-th/0402106.</p> <p>[7] D. Schutte, Phys. Rev. <b>D31</b>, 810 (1985).</p> <p>[8] A. P. Szczepaniak and E. S. Swanson, Phys. Rev. <b>D65</b>, 025012 (2001).</p> <p>[9] D. Epple, H. Reinhardt and W. Schleifenbaum, Phys. Rev. <b>D75</b>, 045011 (2007).</p> <p>[10] W. Schleifenbaum, M. Leder and H. Reinhardt, Phys. Rev. <b>D73</b>, 125019 (2006).</p> <p>[11] H. Reinhardt and D. Epple, Phys. Rev. <b>D76</b>, 065015 (2007).</p> <p>[12] H. Reinhardt, Phys. Lett. <b>101</b>, 061602 (2008).</p> <p>[13] D. R. Campagnari and H. Reinhardt, Phys. Rev. <b>D82</b>, 105021 (2010).</p> <p>[14] D. R. Campagnari and H. Reinhardt, Phys. Lett. <b>B707</b>, 216 (2012).</p> <p>[15] M. Pak and H. Reinhardt, Phys. Lett. <b>B707</b>, 566 (2012).</p> <p>[16] H. Reinhardt, D. R. Campagnari and A. P. Szczepaniak, Phys. Rev. <b>D84</b>, 045006 (2011).</p> <p>[17] J. Heffner, H. Reinhardt and D. R. Campagnari, Phys. Rev. <b>D85</b>, 125029 (2012).</p> <p>[18] H. Reinhardt, J. Heffner Phys. Lett. <b>B718</b>, 672 (2012).</p> <p>[19] A. M. Polyakov, Phys. Lett. <b>B72</b>, 477 (1978).<br/>L. Susskind, Phys. Rev. <b>D20</b>, 2610 (1979).</p> | <p>[20] G. 't Hooft Nucl. Phys. <b>B138</b>, 1 (1978).</p> <p>[21] H. Reinhardt, Phys. Lett. <b>B557</b>, 317 (2003).</p> <p>[22] H. Reinhardt, Nucl. Phys. <b>B503</b>, 505 (1997).</p> <p>[23] O. Jahn and F. Lenz, Phys. Rev. <b>D58</b>, 085006 (1998).<br/>C. Ford, U. G. Mitreuter, T. Tok, A. Wipf and J. M. Pawłowski, Annals Phys. <b>269</b>, 26 (1998).</p> <p>[24] F. Marhauser and J. M. Pawłowski, arXiv:0812.1144 [hep-ph].</p> <p>[25] J. Braun, H. Gies and J. M. Pawłowski, Phys. Lett. <b>B684</b>, 262 (2010).</p> <p>[26] N. Weiss, Phys. Rev. <b>D24</b>, 475 (1981).</p> <p>[27] M. Engelhardt and H. Reinhardt, Phys. Lett. <b>B430</b>, 161 (1998).</p> <p>[28] L. Fister and J. M. Pawłowski, arXiv:1301.4163 [hep-ph].</p> <p>[29] S. Weinberg, The quantum theory of fields. Vol. 2. Cambridge, UK: Univ. Pr. (1996) 489 P.</p> <p>[30] J. Greensite and S. Olejnik, AIP Conf. Proc. <b>1343</b>, 203 (2011)</p> <p>[31] D. Karabali, C. -j. Kim and V. P. Nair, Phys. Lett. <b>B434</b>, 103 (1998).</p> <p>[32] J. Greensite et al., Phys. Rev. <b>D83</b>, 114509 (2011).</p> <p>[33] S. Pokorski, Gauge Field Theories. Cambridge, Uk: Univ. Pr. (1987) 394 P.</p> <p>[34] N. H. Christ and T. D. Lee, Phys. Rev. <b>D22</b>, 939 (1980).</p> <p>[35] J. Taylor, Nucl. Phys. <b>B33</b>, 436 (1971).</p> <p>[36] G. Burgio, M. Quandt, H. Reinhardt, Phys. Rev. Lett. <b>102</b>, 032002 (2009).</p> <p>[37] V. Gribov, Nucl. Phys. <b>B139</b>, 1 (1978).</p> <p>[38] G. Burgio, Private communication.</p> |
|---|--|